© 2020. Published by The Company of Biologists Ltd | Journal of Experimental Biology (2020) 223, jeb216390. doi:10.1242/jeb.216390

RESEARCH ARTICLE

Rainbow trout slow myoblast cell culture as a model to study slow skeletal muscle, and the characterization of *mir-133* and *mir-499* families as a case study

Bruno Oliveira da Silva Duran[1], Maeli Dal-Pai-Silva[1,*] and Daniel Garcia de la serrana[2,3]

ABSTRACT

Muscle fibres are classified as fast, intermediate and slow. *In vitro* myoblast cell culture model from fast muscle is a very useful tool to study muscle growth and development; however, similar models for slow muscle do not exist. Owing to the compartmentalization of fish muscle fibres, we have developed a slow myoblast cell culture for rainbow trout (*Oncorhynchus mykiss*). Slow and fast muscle-derived myoblasts have similar morphology, but with differential expression of slow muscle markers such as *slow myhc*, *sox6* and *pgc-1α*. We also characterized the *mir-133* and *mir-499* microRNA families in trout slow and fast myoblasts as a case study during myogenesis and in response to electrostimulation. Three *mir-133* (*a-1a*, *a-1b* and *a-2*) and four *mir-499* (*aa*, *ab*, *ba* and *bb*) paralogues were identified for rainbow trout and named base on their phylogenetic relationship to zebrafish and Atlantic salmon orthologues. *Omy-mir-499ab* and *omy-mir-499bb* had 0.6 and 0.5-fold higher expression in slow myoblasts compared with fast myoblasts, whereas *mir-133* duplicates had similar levels in both phenotypes and little variation during development. Slow myoblasts also showed increased expression for *omy-mir-499b* paralogues in response to chronic electrostimulation (7-fold increase for *omy-mir-499ba* and 2.5-fold increase for *omy-mir-499bb*). The higher expression of *mir-499* paralogues in slow myoblasts suggests a role in phenotype determination, while the lack of significant differences of *mir-133* copies during culture development might indicate a different role in fish compared with mammals. We have also found signs of sub-functionalization of *mir-499* paralogues after electrostimulation, with *omy-mir-499b* copies more responsive to electrical signals.

KEY WORDS: Slow skeletal muscle, Cell culture, Myoblasts, miRNA, Electrostimulation

INTRODUCTION

Skeletal muscle is the most abundant tissue in teleost fish and can represent up to 60% of total body mass (Johnston, 2001). Skeletal muscle is key for fish propulsion, represents the biggest protein reservoir and is the main product of the aquaculture industry (Johnston, 2001; Sänger and Stoiber, 2001).

Muscle fibre types are classified based on their contractile and metabolic properties as fast, intermediate and slow (Johnston et al., 2004). Fast fibres comprise up to 80–90% of the skeletal muscle and are characterized by fast-twitch, predominantly anaerobic metabolism, low concentrations of myoglobin, mitochondria content and lipids, and low capillary density. The fast fibres are recruited during intense activity, associated with food capture and escape behaviour (Sänger and Stoiber, 2001). Slow fibres comprise 5–20% of muscle mass and are located along the fish body, with a thicker region on the lateral line. They are characterized by having slow-twitch, predominantly aerobic metabolism, high levels of myoglobin, mitochondria content and lipids, and high capillary density (Sänger and Stoiber, 2001). Despite its relatively low abundance, the slow muscle is the main tissue involved in sustained swimming and is critical for middle and long-distance migrations (Bone, 1978; Sänger and Stoiber, 2001). The intermediate fibres have intermediate contractile and metabolic properties between fast and slow fibres and are physically located between these two compartments, representing a very marginal proportion of the total skeletal muscle (Sänger and Stoiber, 2001).

Postembryonic skeletal muscle growth occurs through the activation of myogenic precursor cells (MPCs). MPCs are located between the basal lamina and the sarcolemma of the muscle fibres, and under the absence of stimuli they remain in a quiescent state (then known as satellite cells) (Hollway et al., 2007; Rossi and Messina, 2014; Seger et al., 2011). Satellite cells re-enter the cell cycle in response to different stimuli, such as growth factors, hormones, cytokines, injury, exercise and nutrition, becoming proliferative myoblasts that can either fuse to each other, forming new fibres (hyperplasia), or fuse to pre-existent fibres, contributing to their growth in size (hypertrophy) (Johnston, 2006; Johnston et al., 2011), a process globally known as myogenesis. The establishment of the fish fast myoblast cell culture model has helped to characterize the molecular networks controlling myogenesis (Bower and Johnston, 2010b; Garcia de la serrana and Johnston, 2013; Johnston et al., 2011). The *in vitro* model recapitulates the main stages of the myogenesis, starting with round quiescent cells, followed by proliferative myoblasts and differentiating myotubes (Gabillard et al., 2010; Vélez et al., 2016). Myoblast cell culture facilitates the study of the molecular networks involved in muscle formation in response to specific inputs, such as growth factors and nutrition (Duran et al., 2015, 2019; Garcia de la serrana and Johnston, 2013; Johnston et al., 2011; Vélez et al., 2014). The compartmentalization of skeletal muscle in fish makes it possible to isolate myoblasts from fast and slow muscle, something very difficult in mammals owing to the mixture of fast and slow fibres (Schiaffino and Reggiani, 2011). Until now, the myoblast cell culture had only been developed for fast skeletal muscle, and a similar model for slow muscle was not established.

[1]São Paulo State University (UNESP), Institute of Biosciences, Department of Morphology, Botucatu 18618-689, São Paulo, Brazil. [2]University of St Andrews, Scottish Oceans Institute, School of Biology, St Andrews, Fife KY16 8LB, UK. [3]University of Barcelona, Faculty of Biology, Department of Cell Biology, Physiology and Immunology, 08028 Barcelona, Spain.

*Author for correspondence (maeli.dal-pai@unesp.br)

M.D.-P.-S, 0000-0001-7269-9197

Received 14 October 2019; Accepted 17 December 2019

Journal of Experimental Biology (2020) 223, jeb216390. doi:10.1242/jeb.216390

The teleost lineage underwent a specific whole genome duplication (WGD) around 450–320 million years ago (Mya) (Jaillon et al., 2004). As a result, several signalling pathways and molecular networks had some of their components expanded with multiple paralogue copies. It has been estimated that approximately 15–21% of the duplicated paralogues originated during the WGD have been retained (Garcia de la serrana et al., 2014b). In addition, the salmonid lineage went through an additional WGD around 75 Mya with an estimated 50% paralogue retention (Macqueen and Johnston, 2014; Macqueen et al., 2010, 2013). Paralogue genes can be retained after a WGD through three main mechanisms: sub-functionalization (each paralogue retains part of the original function of the ancestral gene), neo-functionalization (paralogue acquires a different function from the ancestral gene) or redundancy (multiples copies of a gene confer some advantage) (Bower and Johnston, 2010a; Garcia de la serrana and Johnston, 2013; Garcia de la serrana et al., 2014b, 2017; Maere and Van de Peer, 2010).

There is also evidence of microRNA (miRNA) families expanded after the teleost WGD (Berthelot et al., 2014). The primary function of these types of small noncoding RNAs (ncRNA) is the post-transcriptional regulation of gene expression, promoted by translational inhibition and decay of target messenger RNAs (mRNAs) (Ge and Chen, 2011). miRNAs play an orchestrated role in the regulation of multiple targets, controlling several signalling pathways and biological functions (Goljanek-Whysall et al., 2012; van Rooij et al., 2008). Based on the high conservation observed in miRNAs among vertebrates, it can be anticipated that a considerable set of mRNAs are under the modulation by miRNAs in teleosts (Bizuayehu and Babiak, 2014). Some miRNAs such as *mir-1*, *mir-133*, *mir-206* and *mir-499* are specifically or highly expressed in cardiac and/or skeletal muscles, and are involved in myogenesis, myoblast proliferation, differentiation, fibre type specification and muscle regeneration (Chen et al., 2006; Ge and Chen, 2011; van Rooij et al., 2009). Previous studies in pacu (*Piaractus mesopotamicus*) showed that fast and slow muscles have different miRNA expression patterns, as was the case of *miR-499*, which exhibited higher levels of transcription in slow muscle (Duran et al., 2015), suggesting its involvement in the specification and maintenance of slow-twitch phenotype as previously observed in mammals (McCarthy, 2011; van Rooij et al., 2009). In such a context, the innervation pattern has been suggested to be essential for muscle fibre type specification; a tonic and low-frequency neural stimulation induces the slow phenotype, whereas a phasic and high-frequency neural stimulation promotes the fast phenotype (Chin et al., 1998; Olson and Williams, 2000). In the past years, studies have shown that muscle fibre neural activation can be recreated by electrical pulse stimulation (EPS) of cultured skeletal muscle cells (Fujita et al., 2007; Marotta et al., 2004; Thelen et al., 1997). EPS models are useful to investigate adaptive responses of skeletal muscle cells to different patterns of contractile activity, for instance the study of molecular and cellular mechanisms during simulation of resistance or endurance training (Burch et al., 2010; Nedachi et al., 2008; Nikolić et al., 2012; Silveira et al., 2006). Therefore, the electrostimulation represents an important tool with which to investigate the roles of molecules involved with the regulation of muscle growth and phenotype, such as the miRNAs.

In the present work, we established a slow muscle myoblast cell culture from rainbow trout (*Oncorhynchus mykiss*) (Cleveland and Weber, 2010; Gabillard et al., 2010; Montserrat et al., 2007a; Seiliez et al., 2008) and used it to characterize the *mir-133* and *mir-499* families during slow and fast myoblast development and in response to EPS applied on slow muscle cell cultures.

MATERIALS AND METHODS

Ethics statement and animals

All experiments and procedures were approved by the Animal Welfare and Ethics Committee (AWEC) of the University of St Andrews and were carried out in accordance with relevant guidelines and regulations. Rainbow trout [*Oncorhynchus mykiss* (Walbaum 1792)] juveniles (10–15 g) were obtained from Frandy Farm (Gleneagles, Scotland) and transported to the Scottish Oceans Institute aquarium facilities (University of St Andrews). Animals were evenly distributed in duplicated 200 litre fibreglass tanks, maintained in a freshwater re-circulatory system at a temperature between 12 and 15°C and fed *ad libitum* daily with commercial diet provided by the same farm of origin. Trout were humanely killed by head dislocation followed by the destruction of the brain with a scalpel according to Schedule 1 protocols as described in the Animals (Scientific Procedures) Act 1986 (Home Office Code of Practice. HMSO: London, January 1997).

Myoblast cell culture

A total of four independent myoblast cell cultures were performed as previously described (Fauconneau and Paboeuf, 2000). Briefly, fast muscle samples were collected from the epaxial region and slow muscle was carefully dissected around the lateral line (n=14–16 fish per culture until reaching a total of 20 g per tissue). Fast and slow muscles were mechanically dissociated with scalpels and enzymatically digested with 0.2% type I collagenase (Sigma-Aldrich) and 0.1% trypsin (Sigma-Aldrich). Cells were filtered through 40 and 100 µm cell strainers (Thermo Fisher Scientific) to remove any debris. After several washes, cells were resuspended in Dulbecco's modified Eagle's medium (DMEM, 9 mmol l^{-1} $NaHCO_3$, 20 mmol l^{-1} Hepes, pH 7.4; Sigma-Aldrich) with 10% fetal bovine serum (FBS) and 1% antibiotic mixture (Sigma-Aldrich). After cell counting in a Neubauer chamber, cells were diluted to a final concentration of 2×10^6 cells ml^{-1} and seeded in poly-L-lysine and laminin pre-treated 6-well plates. Slow and fast myoblasts were maintained at 18°C for a total period of 12 days. Culture media were changed daily, and myoblast morphology was regularly monitored using a Leica DM IL Inverted Microscope coupled with the Leica DFC320 Digital Camera system. Total RNA was extracted from cells at days 2, 4, 6, 8, 10 and/or 12.

Electrical pulse stimulation (EPS)

Electrostimulation was performed using a C-Pace EP Cell Culture Stimulator in conjunction with the C-Dish Electrode Assemblies (IonOptix). Myoblasts were electro-stimulated daily from day 4 of culture until day 10 following three different protocols: control plate (CTR; non-treated cells), acute treatment (A-EPS; cells treated with acute and high-frequency stimulation, simulating fast muscle innervation) and chronic treatment (C-EPS; cells treated with chronic and low-frequency stimulation, simulating slow muscle innervation). The acute treatment was applied for 15 min and the myoblasts were submitted to pulse trains of 10 Hz and 30 V for 10 ms, given every fifth second. The chronic treatment was applied for 2 h and the myoblasts were submitted to pulse trains of 1 Hz and 30 V for 2 ms. The myoblasts were electro-stimulated in serum-free DMEM and remained resting for 10 min before adding fresh medium. RNA extractions for days 6, 8 and 10 of cell culture were performed 2 h after the EPS.

miRNA phylogenetic analysis

Initially, the precursor sequences of miRNAs *mir-133*, *mir-499* and *mir-206* (an miRNA also highly expressed in muscle; Ge and Chen,

2011; Ma et al., 2015) were obtained from the zebrafish (*Danio rerio*) genome using the Ensembl Genome Browser 89 (http://www.ensembl.org/index.html). Zebrafish miRNAs were used as query against the available rainbow trout genome in Genoscope (https://www.genoscope.cns.fr/trout/) (Berthelot et al., 2014). Identified trout orthologues were initially named as *omy-mir-133* and *omy-mir-499* until their identity was phylogenetically established. Orthologues for *mir-133* and *mir-499* precursor sequences (pre-miRNA) from different teleosts (*Astyanax mexicanus*, *D. rerio*, *Gasterosteus aculeatus*, *Oreochromis niloticus*, *Oryzias latipes*, *Takifugu rubripes*, *Tetraodon nigroviridis*) and mammals (*Homo sapiens*, *Mus musculus*, *Pan troglodytes* and *Rattus norvegicus*) were retrieved from the Ensembl database. In addition, pre-miRNA orthologues for Atlantic salmon (*Salmo salar*) and coho salmon (*Oncorhynchus kisutch*) were also obtained from SalmoBase (https://salmobase.org/) (Samy et al., 2017) and NCBI (http://www.ncbi.nlm.nih.gov). The pre-miRNA sequences (Table S1) were aligned using MAFFT version 7 (http://mafft.cbrc.jp/alignment/server/), while MEGA7 software (Kumar et al., 2016) was used to estimate the best evolutionary model from aligned sequences. Bayesian MCMC (Markov chain Monte Carlo) phylogenetic trees following a Yule speciation process model and UPGMA (unweighted pair group method with arithmetic mean) starting tree were generated for each alignment using BEAST v1.7.4 software (Drummond et al., 2012) with 10,000,000 seeds. Final Bayesian trees were generated using TreeAnnotator v.1.7 with a burn-in value of 1000. All trees were visualized and edited using FigTree v.1.4.2 (http://tree.bio.ed.ac.uk/software/figtree/).

RNA extraction and reverse transcription

Total RNA was extracted using TRIsure™ (Bioline Reagents), according to the manufacturer's recommendations, and stored at −80°C for further analysis. Total RNA was quantified by spectrophotometry using a Nanodrop (ND1000) (Thermo Fisher Scientific) while integrity was evaluated by 1% ethidium bromide agarose gel electrophoresis. All samples had 280/260 nm and 230/260 nm ratios above 1.8, indicating high-quality RNA. A total of 224 ng of total RNA per sample was reverse transcribed using the miScript II RT Kit and the QuantiTec Reverse Transcription Kit (Qiagen, Germany), following the manufacturer's guidelines. The resulting cDNA was used for quantitative real-time PCR (qPCR).

Primer design

Primers for rainbow trout *slow myosin heavy chain* (*smyhc*), *fast myosin heavy chain* (*fmyhc*), *sry sex determining region Y-box 6* (*sox6*), *six homeobox 1* (*six1*), *insulin-responsive glucose transporter type 4* (*glut4*), *late endosomal/lysosomal adaptor, mapk and mtor activator 3* (*lamtor3*), *ras related GTP binding D* (*ragd*), *regulatory associated protein of mtor complex 1* (*rptor*), *muscle atrophy f-box protein* (*mafbx/fbxo32*), *peroxisome proliferator-activated receptor gamma coactivator 1 alpha* (*pgc-1α*), *creatine kinase, m-type a* (*ckma*), *creatine kinase, m-type b* (*ckmb*), *myogenin* (*myog*), *ribosomal protein L13* (*rpl13*) and *ribosomal protein L19* (*rpl19*), and paralogues of *omy-mir-133* (133a-1a, 133a-1b and 133a-2), *omy-mir-499* (499aa, 499ab, 499ba, 499bb), *omy-mir-206-1* and *U6 snRNA* (*U6 small nuclear RNA*) were designed using Primer3 v.0.4.0 (Koressaar and Remm, 2007; Untergasser et al., 2012) (Table S2). The precursor sequences from each rainbow trout miRNA were used to design the forward and reverse primers in regions with low similarity in order to amplify individual paralogues (primers for *omy-mir-499aa* amplified both *499aa* and *499ab* copies, resulting in a global *omy-mir-499a* expression (aa+ab). Primers for miRNA were designed to work at 60°C and amplify 60–100 bp regions while primers for mRNA were designed to work at 60°C and amplify 50–200 bp regions. Any possible hairpin, self-dimer or cross-dimer structures formed by the primer pairs were estimated using NetPrimer software (Premier Biosoft).

Quantitative real-time PCR (qPCR)

All qPCR performed was compliant with the Minimum Information for Publication of Quantitative Real Time PCR experiments (MIQE) guidelines (Bustin et al., 2009). Each qPCR reaction contained 6 µl of diluted cDNA (1:40), 7.5 µl of SensiFAST™ SYBR® master mix (Bioline Reagents) and 1.5 µl of 500 nmol l^{-1} forward/reverse primer mix. The reactions were performed in duplicate under the following conditions: one cycle at 95°C for 2 min followed by 40 cycles of denaturation at 95°C for 5 s and annealing/extension at 65°C for 20 s in an MX3005P Real Time PCR System (Agilent Technologies). The specificity of each primer set was confirmed by the presence of a single-peak dissociation curve. Gene expression was estimated using the $2^{-\Delta\Delta C_t}$ method (Livak and Schmittgen, 2001). Different housekeeping genes were tested (*rpl13*, *rpl19*, *omy-mir-206-1* and *U6 snRNA*) and NormFinder software (Andersen et al., 2004) was used to identify the optimal normalization gene for miRNA and mRNA expression. *Rpl13* and *omy-mir-206-1* were identified as the most suitable housekeeping genes for mRNA and miRNA expression, respectively. The secondary structure of the identified miRNA precursor sequences was predicted using the RNAfold WebServer (Gruber et al., 2008) (Fig. S1).

Statistical analysis

Statistical analyses were performed using RStudio v1.0.136 (https://rstudio.com/) and statistical significance was set at 5% ($P<0.05$). The normality of the expression data was tested using the Shapiro–Wilk test. When the normality assumption was fulfilled, data were analyzed using a two-way ANOVA followed by a *post hoc* Tukey's honestly significant difference (HSD) test, with the tissue of origin (tissue) and the day of development (development) as factors. When the normality assumption was not fulfilled, data were transformed using the Box–Cox power transformation approach (Box and Cox, 1964) and analyzed as described. In addition, miRNA expression data from slow and fast myoblast comparison were analyzed using the unpaired *t*-test with tissue as a factor, and miRNA expression data from EPS treatments were analyzed using a one-way ANOVA followed by a *post hoc* Dunn's test, with treatment as a factor for the analysis. Pearson's correlation was used to access interesting relationships between evaluated genes. All graphs were constructed using the ggplot2 R package (Wickham, 2016).

RESULTS

Myoblast cell culture

Fast myoblast cell culture requires small juveniles (3–5 g) in order to maximize the number of myoblasts obtained (Castillo et al., 2002, 2006; Garcia de la serrana and Johnston, 2013; Montserrat et al., 2007b). However, slow muscle extraction requires larger animals in order to be able to discriminate between tissues and to dissect pure slow muscle. We found that rainbow trout around 15 g of body mass yield enough fast and slow myoblasts from individual animals to perform the experiment described in the present study (Fig. 1A). Compared with fast skeletal muscle, slow muscle extraction requires a harder mechanical dissociation, does not change DMEM colour (lactate from fast muscle turns it orange) and originates a top layer of

Journal of Experimental Biology (2020) 223, jeb216390. doi:10.1242/jeb.216390

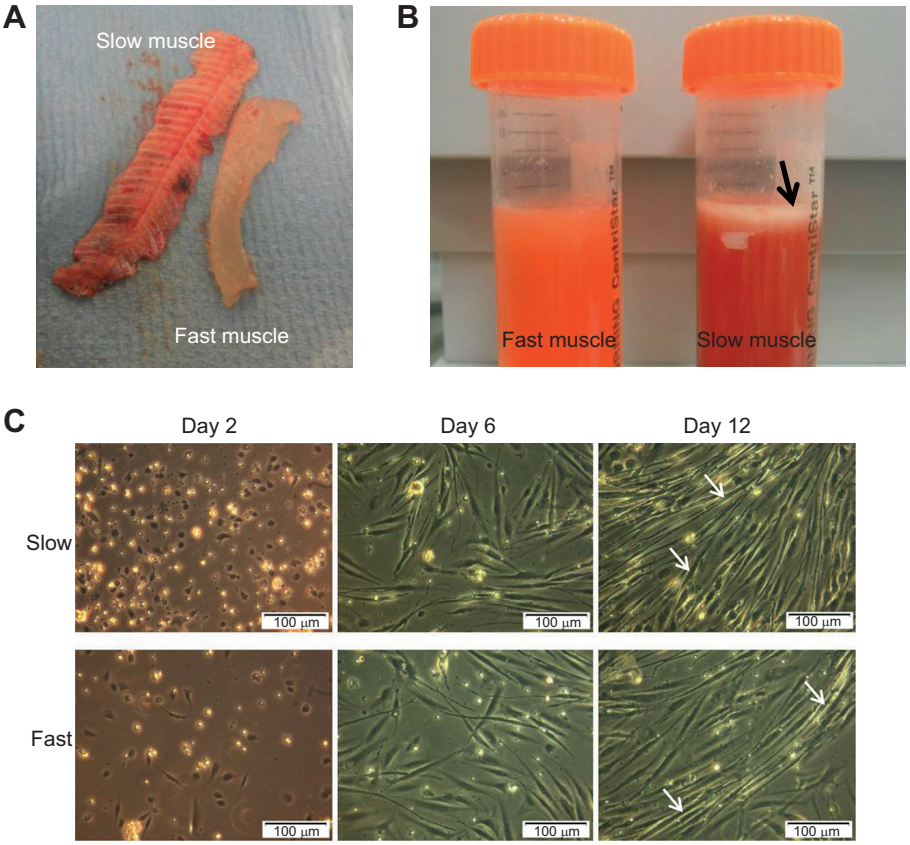

Fig. 1. Rainbow trout fast and slow myoblast cell culture establishment. (A) Slow muscle strips were carefully extracted from the surroundings of the lateral line and any remnants of fast muscle were removed to avoid cross-contamination. Fast muscle samples were collected from the epaxial region after slow muscle removal. (B) Fast muscle extraction tube showing the DMEM slightly orange because of pH reduction by lactic acid, and slow muscle extraction tube with a top layer of lipids (black arrow). (C) Rainbow trout fast and slow myoblasts at days 2, 6 and 12 of development (20× magnification). Myotubes are indicated by white arrows.

fat that, if not removed, would reduce the efficiency of extraction (Fig. 1B, black arrow). At the end of the extraction protocol, slow skeletal muscle consistently yielded more cells per gram of tissue than fast skeletal muscle (data not shown). Slow and fast myoblasts were morphologically very similar with equivalent developmental stages during the culture progression: round mononucleated cells between days 1 and 2, proliferative myoblasts between days 3 and 7 and distinctive myotubes between days 8 and 12 (Fig. 1C, white arrows).

Characterization of slow muscle-derived myoblast cell culture

Myogenic nature of the cell cultures was confirmed by the expression of the muscle-specific transcription factor *myogenin* (*myog*) during the myotube formation phase (Fig. S2) (Johnston, 2006). The phenotype of slow-derived myoblasts was confirmed by analyzing the expression of *smyhc*, *fmyhc*, *six1* and *sox6* during the culture progression (Fig. 2). Expression of *fmyhc* and *smhyc* was significantly different between cell cultures (tissue $P<0.001$ and development $P<0.001$) (Fig. 2A,B). The abundance of *fmyhc* was 2.5-fold higher in fast muscle cell culture between days 8 and 12 (Fig. 2B), while *smyhc* showed a >12-fold increase in slow muscle myotubes (Fig. 2A). The expression levels of the *six1* and *sox6* transcription factors were higher in fast than slow myoblast cell culture (tissue $P<0.001$ for both genes) (Fig. 2C,D). Both transcription factors had maximal abundance between days 6 to 10 (development $P<0.001$ for both genes) (Fig. 2C,D).

In order to investigate metabolic differences between tissues, we studied the expression of genes related to protein balance (*lamtor3*, *ragd*, *rptor* and *mafbx*), glucose uptake (*glut4*) and energy (*pgc1α*, *ckma* and *ckmb*) (Fig. 3). Despite the differences between slow and fast muscle cells not being significant for *glut4*, *lamtor3* and *ragd* (tissue $P=0.58$, 0.22 and 0.63, respectively) (Fig. 3A–C), their transcription was slightly higher in slow cell culture and decreased between days 8 to 12 (Fig. 3A,C). In both tissues, the *mafbx* expression similarly (tissue $P=0.05$) decreased suddenly after day 2 (development $P<0.001$) and remained low until the end of the culture, while *rptor* did not change between tissues (tissue $P=0.53$) or culture development (development $P=0.07$) (Fig. 3D,E). In contrast, *pgc1α* expression was stable during the cell culture (development $P=0.59$) and significantly higher in slow culture (tissue $P<0.001$) (Fig. 3F). The expression pattern of *ckma* and *ckmb* paralogues was very similar between slow and fast muscle cells (tissue $P=0.28$ for *ckma* and $P=0.36$ for *ckmb*), with maximal expression during myotube formation (days 8 to 12) (development $P<0.001$ for both genes) (Fig. 3G,H).

miRNA identification

Several members of the *mir-133* and *mir-499* families were identified for rainbow trout, coho salmon and Atlantic salmon. We used phylogenetic analysis to establish their identity and name them based on the existent zebrafish and salmonid nomenclature. Phylogenetic analysis confirmed the existence of three copies of *mir-133* (Fig. 4) and four of *mir-499* (Fig. 5) in rainbow trout. According to the tree topology, rainbow trout paralogues were named as *omy-mir-133a-1a*, *omy-mir-133a-1b*, *omy-mir-133a-2*, *omy-mir-499aa*, *omy-mir-499ab*, *omy-mir-499ba* and *omy-mir-499bb* (Figs 4 and 5; Table S1). Globally, miRNA sequences were highly conserved, with identities over 92% (Table S3). We also observed that paralogues of the same family had very similar secondary structures while differences between *mir-133* and *mir-499* families were also clear (Fig. S1). Owing to the high

Journal of Experimental Biology (2020) 223, jeb216390. doi:10.1242/jeb.216390

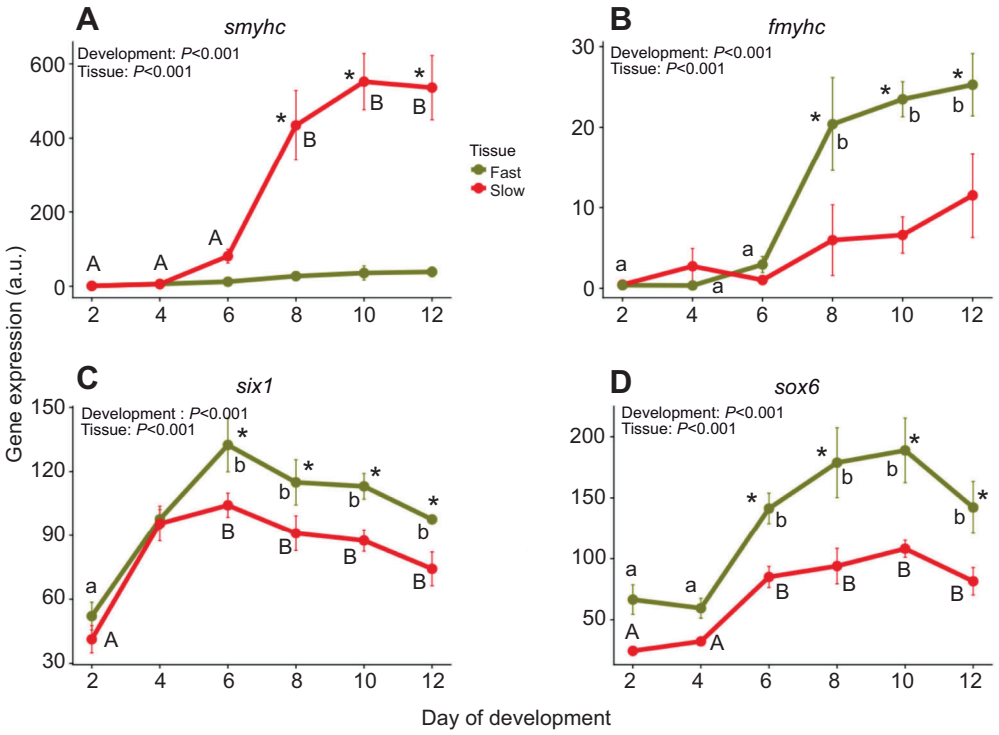

Fig. 2. Rainbow trout fast and slow myoblast cell culture characterization. Gene expression in slow and fast myoblast cell culture at days 2, 4, 6, 8, 10 and 12 of development for (A) *slow myosin heavy chain* (*slow myhc*), (B) *fast myosin heavy chain* (*fast myhc*), (C) *six homeobox 1* (*six1*) and (D) *SRY* (*sex determining region Y*) *box 6* (*sox6*). Values represent means±s.e.m. (*n*=4 independent cell cultures). Data were analyzed using a two-way ANOVA followed by a *post hoc* Tukey's honestly significant difference (HSD) test, with the tissue of origin (tissue) and the day of development (development) as factors. *P*-values of tissue and development are shown. Asterisks indicate significant differences between means of slow and fast myoblast cell cultures, and different letters (uppercase for slow and lowercase for fast) indicate significant differences between means of days of development ($P<0.05$).

degree of identity, the primers designed for *omy-mir-499aa* also amplified the *omy-mir-499ab* copy, and therefore *omy-mir-499aa* paralogue represents the sum of both (*omy-mir-499aa+ab*).

miRNA expression during fast and slow myoblast culture development

Expression of *mir-133* and *mir-499* paralogues was studied in slow- and fast-derived myoblast cell cultures at days 6, 8 and 10 of development (Fig. 6). No significant differences in expression were found for any of the *omy-mir-133* paralogues between slow and fast cell cultures (Fig. 6A–C). Between days 6 to 8, expression was 0.5-fold lower for *omy-mir-499aa+ab* and *omy-mir-499bb* and 0.6-fold lower for *omy-mir-499ab* in fast- compared with slow-derived myocytes (tissue $P<0.01$) (Fig. 6D–G). *Omy-mir-499* copies did not show statistical differences during culture development (development $P=0.62$, 0.88, 0.86 and 0.94 for *omy-mir-499aa+ab*, *omy-mir-499ab*, *omy-mir-499ba* and *omy-mir-499bb*, respectively) (Fig. 6D–G).

Expression of *omy-mir-133* and *omy-mir-499* paralogues in response to electrical stimulation on slow muscle myoblasts were also investigated (Fig. 7). From the *omy-mir-133* family, only *omy-mir-133a-2* transcription significantly increased by 2-fold at day 6 of chronic stimulation (C-EPS group) (treatment $P<0.05$) (Fig. 7A–C). The expression of *omy-mir-499ab* at day 6 was 0.5-fold lower in C-EPS treated cells than in the CTR group (treatment $P<0.05$) (Fig. 7E). *Omy-mir-499ba* transcription was 7-fold higher at day 6 and 4-fold higher at day 8 (treatment $P<0.001$) in C-EPS treated cells compared with in the CTR group (Fig. 7F). The chronic stimulation also increased expression of the *omy-mir-499bb* paralogue, by 2.5-fold at day 6 (treatment $P<0.001$) and by 2-fold at day 8 (treatment $P<0.01$). In addition, *omy-mir-499bb* expression at day 6 was 2.3-fold higher in acute-stimulated myoblasts (A-EPS group) compared with in the CTR group (treatment $P<0.01$) (Fig. 7G).

To complement our results and provide further insight into miRNA paralogue roles, we performed correlation analyses between expression of *omy-mir-133*, *omy-mir-499*, *smyhc*, *fmyhc* and *sox6* (Fig. S3). It is interesting to highlight the negative correlation between *omy-mir-499* paralogues and *sox6* ($\rho=-0.38$ for *omy-mir-499aa+ab* versus *sox6*; $\rho=-0.5$ for *omy-mir-499ba* versus *sox6*; $\rho=-0.51$ for *omy-mir-499bb* versus *sox6*), all of them significant (Fig. S3).

DISCUSSION

In the present study, we established a viable teleost slow myoblast cell culture, similar to the fast myoblast cell culture with some considerations: (1) the slow muscle is much firmer and very easy to lose during washes; (2) a layer of fat is formed during extraction that should be removed in order to increase cell yield; (3) after enzymatic digestion, slow muscle is especially rich in tissue debris and should be carefully filtered and washed; and (4) for an equivalent amount of tissue, slow muscle yields 43% more myoblasts than fast muscle (based on Neubauer chamber counting; data not shown). Unless the experimental design requires samples from the same animals, we recommend using small juveniles to extract fast skeletal muscle and larger animals for slow skeletal muscle. The difference in the number of myoblasts extracted from both tissues is in agreement with previous studies reporting a higher proportion of satellite cells in slow fibres (Gibson and Schultz, 1982) but with equivalent development stages as described for fast myoblast cell cultures

Journal of Experimental Biology (2020) 223, jeb216390. doi:10.1242/jeb.216390

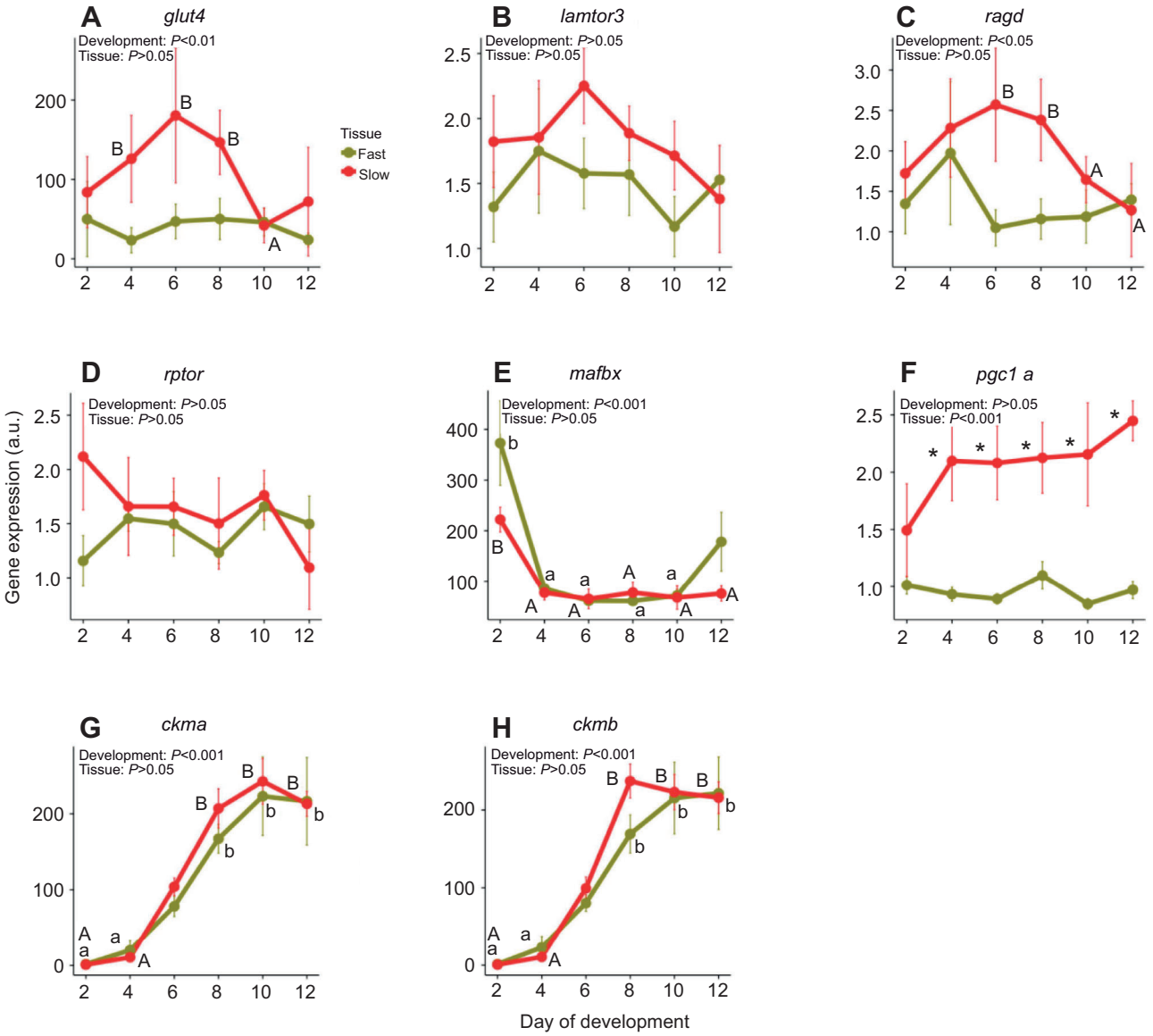

Fig. 3. Muscle regulatory signaling components in rainbow trout fast and slow myoblast cell culture. Gene expression in slow and fast myoblast cell culture at days 2, 4, 6, 8, 10 and 12 of development for (A) *insulin-responsive glucose transporter type 4* (*glut4*), (B) *late endosomal/lysosomal adaptor, mapk and mtor activator 3* (*lamtor3*), (C) *ras related GTP binding D* (*ragd*), (D) *regulatory associated protein of mtor complex 1* (*rptor*), (E) *muscle atrophy f-box protein* (*mafbx*), (F) *peroxisome proliferator-activated receptor gamma coactivator 1 alpha* (*pgc1α*), (G) *creatine kinase, m-type a* (*ckma*) and (H) *creatine kinase, m-type b* (*ckmb*). Values represent means±s.e.m. (*n*=4 independent cell cultures). Data were analyzed using a two-way ANOVA followed by a *post hoc* Tukey's HSD test, with the tissue of origin (tissue) and the day of development (development) as factors. *P*-values of tissue and development are shown. Asterisks indicate significant differences between means of slow and fast myoblast cell cultures, and different letters (uppercase for slow and lowercase for fast) indicate significant differences between means of days of development (*P*<0.05).

(Fig. 1) (Bower and Johnston, 2010a; Castillo et al., 2006; Garcia de la serrana et al., 2014a).

Despite the morphological similarities between the slow and fast muscle cells, they were phenotypically different, as indicated by the expression profiles of *six1*, *sox6*, *fmyhc* and *smyhc*. Sox6 is a transcription factor that represses the slow fibre phenotype (Hagiwara et al., 2007), whereas Six1, another transcription factor, is required for the determination of the fast phenotype (Bessarab et al., 2008). Our results show that *six1* and *sox6* levels were significantly lower in slow myogenic cells, indicating that the slow program was not repressed (Fig. 2). Slow myogenic cells had a much higher expression of *smyhc* compared with *fmyhc* (Fig. 2). Our results suggest that myoblasts from slow and fast muscle tend to differentiate to the fibre type of the tissue they were extracted from, in agreement with a previous study on birds, where myoblasts extracted from the pectoralis major and anterior latissimus dorsi formed fast and slow myotubes in similar proportions as found in the muscle of origin (Feldman and Stockdale, 1991). It is interesting to note that slow muscle myogenic cells showed unexpectedly high levels of *fmyhc* (Fig. 2), raising questions about the possibility of some degree of phenotypic plasticity, i.e. turning into the fast phenotype in response to endocrine, nutritional or electrical signals.

We analyzed the expression of genes involved in different metabolic processes in order to gain a preliminary idea of the metabolic differences or similarities between slow and fast myoblasts. Many of the genes studied had a higher expression in

Journal of Experimental Biology (2020) 223, jeb216390. doi:10.1242/jeb.216390

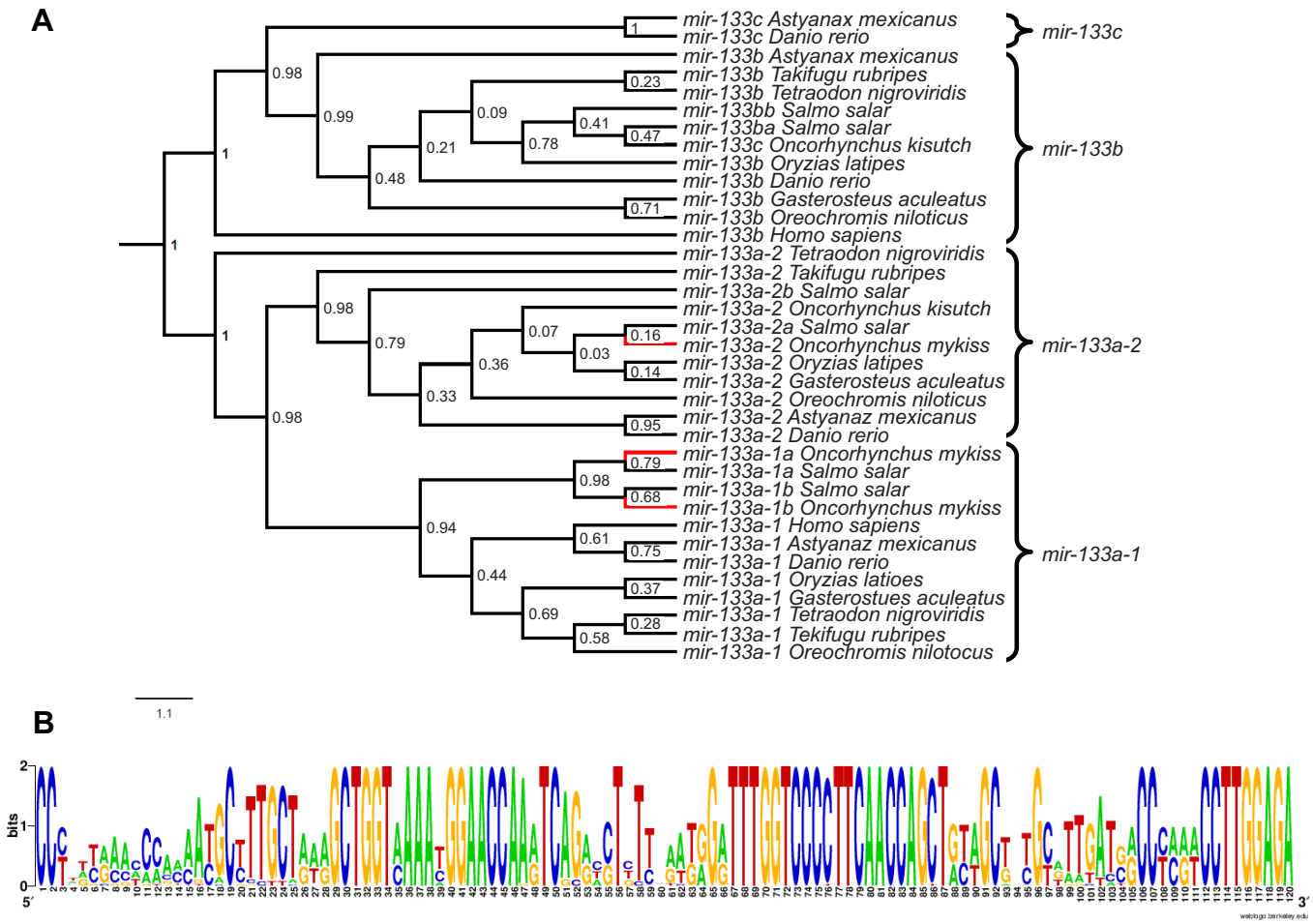

Fig. 4. Teleost fish *mir-133* phylogenetic analysis. (A) Phylogenetic reconstruction of the *mir-133* family using Bayesian methods. The tree was constructed from a high confidence alignment of 36 pre-miRNA sequences and used Hasegawa–Kishino–Yano with gamma distribution (HKY+G) as the best-fitted substitution model. Bootstrap-posterior values are indicated on the node of each branch. Branches in red indicate the *mir-133* copies identified for rainbow trout. (B) Multiple alignment was analyzed on the WebLogo 3 server from University of California, Berkeley, for logo representation of all the miRNAs used for the phylogenetic reconstruction; the *y*-axis represents conservation of nucleotides at that position (height).

the slow myoblasts (*glut4*, *lamtor3*, *ragd* and *pgc1α*), despite only *pgc1α* showing a statistically significant difference (Fig. 3). Pgc1α acts as a co-factor of mitochondrial biogenesis, and it is crucial to maintain slow muscle oxidative metabolism (Chan and Arany, 2014). Moreover, slow fibres might be significantly more insulin-responsive than fast fibres, owing to higher levels of the Glut4 protein (Kern et al., 1990), as inferred by a higher transcription of *glut4* on slow myoblasts. The Lamtor/Rrag GTPases complex has been identified to act as an amino acid sensor and promote Mtor activation, representing an important mechanism through which amino acids stimulate protein synthesis by themselves (Demetriades et al., 2014; Sancak et al., 2010). Despite the similar expression pattern of *rptor* between fast and slow cultures, *lamtor3* and *ragd* had higher transcription in slow myogenic cells (Fig. 3), suggesting a higher contribution of the Lamtor/Rrag GTPases complex to protein synthesis. The idea of an increase in protein synthesis during the progression of the cell culture is further supported by the expression of the E3 ubiquitin ligase *mafbx*, which was strongly inhibited in both tissues (Fig. 3) (Sandri, 2008).

We also used slow and fast muscle cell cultures as a model to characterize *mir-133* and *mir-499* families during differentiation and in response to electrostimulation. The miRNA mature sequences and secondary structures are highly conserved among different vertebrate species and between paralogues of the same family (Bizuayehu and Babiak, 2014). Phylogenetic analysis confirmed the identity of three *mir-133* (*omy-mir-133a-1a*, *omy-mir-133a-1b* and *omy-mir-133a-2*) and four *mir-499* (*omy-mir-499aa*, *omy-mir-499ab*, *omy-mir-499ba* and *omy-mir-499bb*) in rainbow trout, as expected after successive WGD. It is also interesting to highlight that rainbow trout seems to lack *mir-133b* and *-133c*, indicating a species-specific loss.

The *omy-mir-133* paralogues had similar levels of expression between fast and slow myoblast cell cultures, with very little variation during development (Fig. 6). *mir-133* has been described to be involved in muscle development by preventing myoblast differentiation and enhancing myoblast proliferation (Chen et al., 2006; Yu et al., 2014), which disagrees with the lack of transcriptional variation found in our study. Because *mir-133* levels were unaffected in almost all conditions, expression of the target *srf* (*serum responsive factor*) was not determined in the present study. It might be possible that *mir-133* has a different role in fish than that suggested in mammals, or that relevant changes occurred before day 6 of development, which was not included in the present work and would need further investigation.

The *omy-mir-499* paralogues had higher abundance in slow myoblasts (Fig. 6), which is in agreement with the role of this

Journal of Experimental Biology (2020) 223, jeb216390. doi:10.1242/jeb.216390

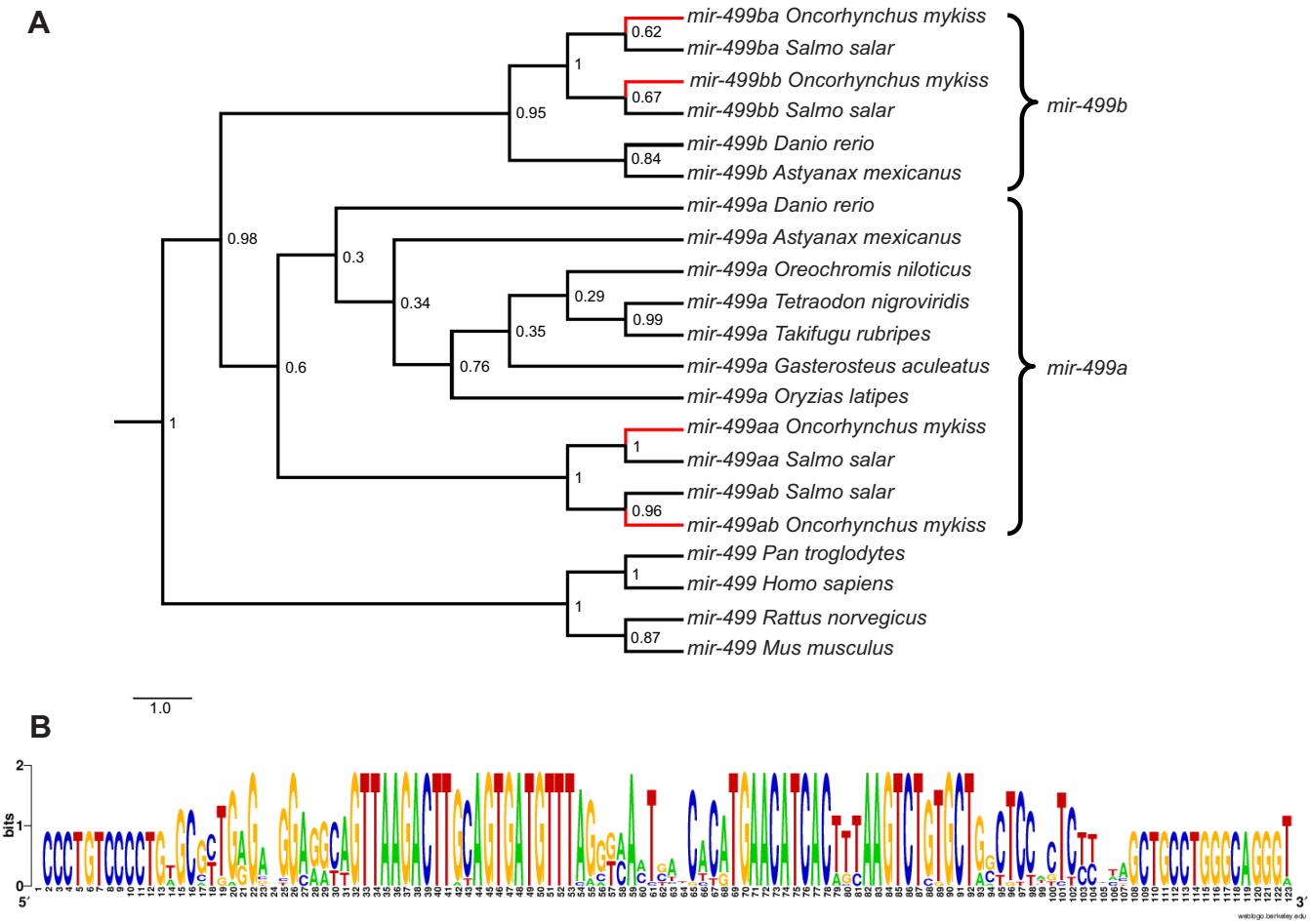

Fig. 5. Teleost fish *mir-499* phylogenetic analysis. (A) Phylogenetic reconstruction of the *mir-499* family using Bayesian methods. The tree was constructed from a high confidence alignment of 21 pre-miRNA sequences and used HKY+G as the best-fitted substitution model. Bootstrap-posterior values are indicated on the node of each branch. Branches in red indicate the *mir-499* copies identified for rainbow trout. (B) Multiple alignment was analyzed on WebLogo 3 server from University of California, Berkeley, for logo representation of all the miRNAs used for the phylogenetic reconstruction; the *y*-axis represents conservation of nucleotides at that position (height).

miRNA promoting the slow fibre type phenotype (van Rooij et al., 2009; Wang et al., 2011). In both mammals (McCarthy et al., 2009; van Rooij et al., 2009) and teleost fish (Duran et al., 2015; Nachtigall et al., 2015; Wang et al., 2011), *miR-499* mediates the translational repression of *sox6*, a putative target involved in the maintenance of the fast-twitch phenotype through the repression of slow-twitch-specific genes, such as *slow myosin heavy chain 1* (von Hofsten et al., 2008). Our results show a negative correlation between several *omy-mir-499* paralogues and *sox6*, suggesting that a similar mechanism might be in place in slow myoblast cell culture. These data are corroborated by the positive correlation between *omy-mir-499ab* and *smyhc*, as opposed to *omy-mir-499bb* and *fmyhc* (Fig. S3). In response to electrical stimulation, both *mir-499b* paralogues (*omy-mir-499ba* and *omy-mir-499bb*) increased their transcription after C-EPS treatment, indicating that *mir-499b* paralogues could be more susceptible to long-term electrical stimuli than *mir-499a* duplicates. Results from the C-EPS treatment suggest that the *mir-499b* paralogues might have an active role in slow fibre type specification and maintenance. However, considering the decreased expression of *omy-mir-499ab* at day 6 and a tendency of increased expression of *omy-mir-499aa+ab* at day 10 in C-EPS myoblasts (Fig. 7), another possibility could be that *omy-mir-499b* paralogues have an early role in slow phenotype determination, while *omy-mir-499a* copies may act in the late stage of myotube formation. Both possibilities suggest the sub-functionalization of *omy-mir-499* paralogues, as a result of the teleost-specific WGD (Jaillon et al., 2004). Our study shows that *omy-mir-499b* paralogues probably retained only part of the original function of the *omy-mir-499* gene, appearing to be more responsive to electrical signals and/or more involved in phenotype specification at early stages compared with *omy-mir-499a* copies. Evidence of the sub-functionalization of *myod1* (*myogenic differentiation factor 1*) paralogues was also observed during myotube formation of Atlantic salmon muscle cells, with *myod1a* primarily expressed during cell differentiation and *myod1b* and *1c* especially expressed during cell proliferation (Bower and Johnston, 2010a). Given the increased expression of *mir-499b* copies in the C-EPS group, we can conclude that chronic and slow-frequency stimulation enhanced the slow phenotype in cell culture and could be used in skeletal muscle fibre type studies.

The slow myoblast cell culture represents an interesting and useful *in vitro* model with which to study skeletal muscle. Particularities in processes such as muscle development, wasting and regeneration can be addressed in this system, in addition to

Journal of Experimental Biology (2020) 223, jeb216390. doi:10.1242/jeb.216390

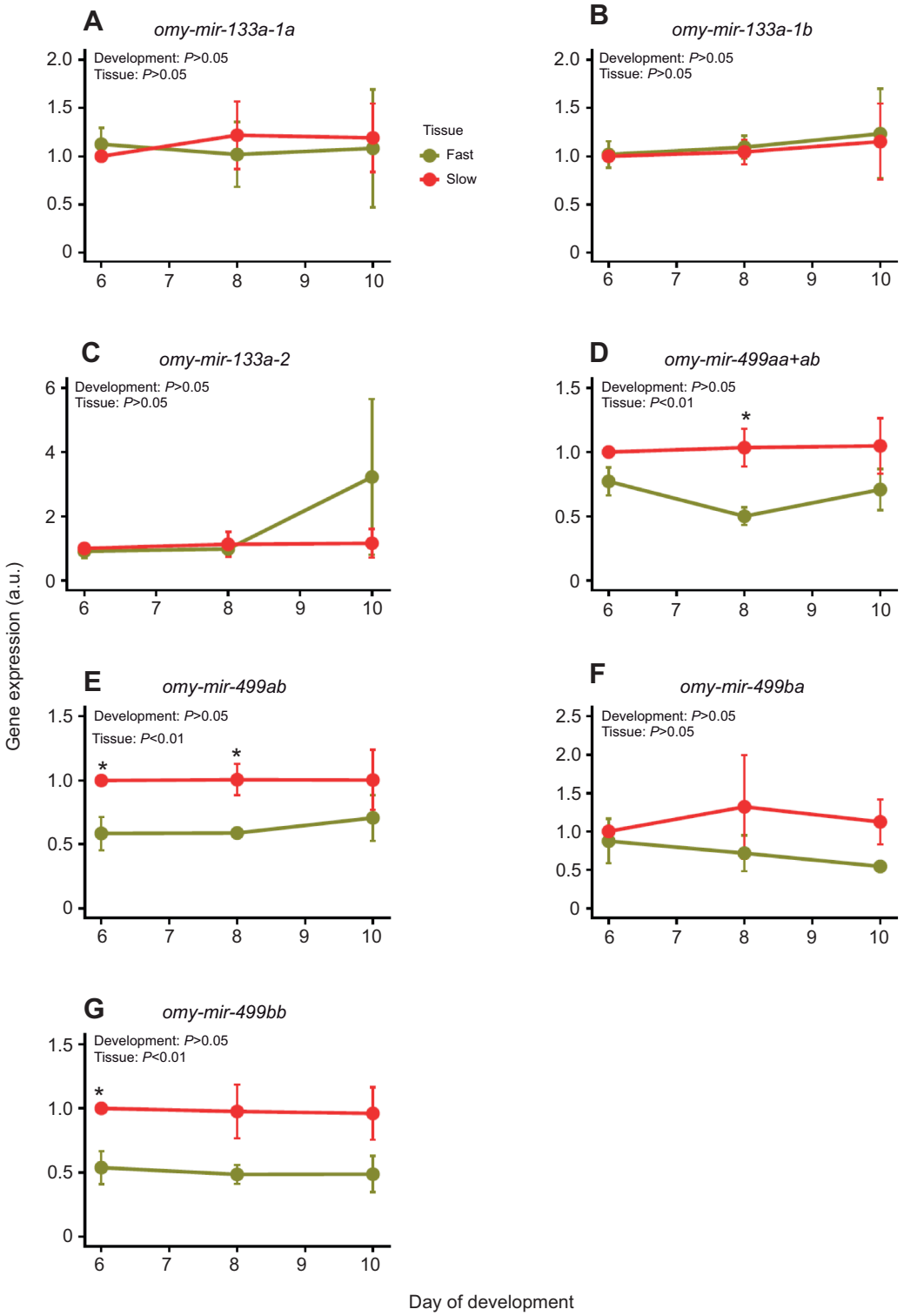

Fig. 6. *miR-133* and *miR-499* paralogue expression in rainbow trout fast and slow myoblast cell culture. Gene expression in slow and fast myoblast cell culture at days 6, 8 and 10 of development for (A) *omy-mir-133a-1a*, (B) *omy-mir-133a-1b*, (C) *omy-mir-133a-2*, (D) *omy-mir-499aa+ab*, (E) *omy-mir-499ab*, (F) *omy-mir-499ba* and (G) *omy-mir-499bb*. Values represent means±s.e.m. (n=4 independent cell cultures). Data were analyzed using an unpaired t-test with the tissue of origin (tissue) as factor. P-values of tissue and day of development (development) are shown. Asterisks indicate significant differences between means of slow and fast myoblast cell cultures (P<0.05).

modulation of muscle fibre phenotypes, such as studies investigating exercise and phenotypic plasticity. The cultured slow myoblasts offer the possibility for future manipulative and pharmacological experiments, including gain or loss of function assays that may provide new information about the roles of individual genes or signaling molecules. The next steps in the characterization of *mir-133* and *mir-499* paralogues in rainbow trout include the use of miRNA inhibitors and mimics to alter their

Journal of Experimental Biology (2020) 223, jeb216390. doi:10.1242/jeb.216390

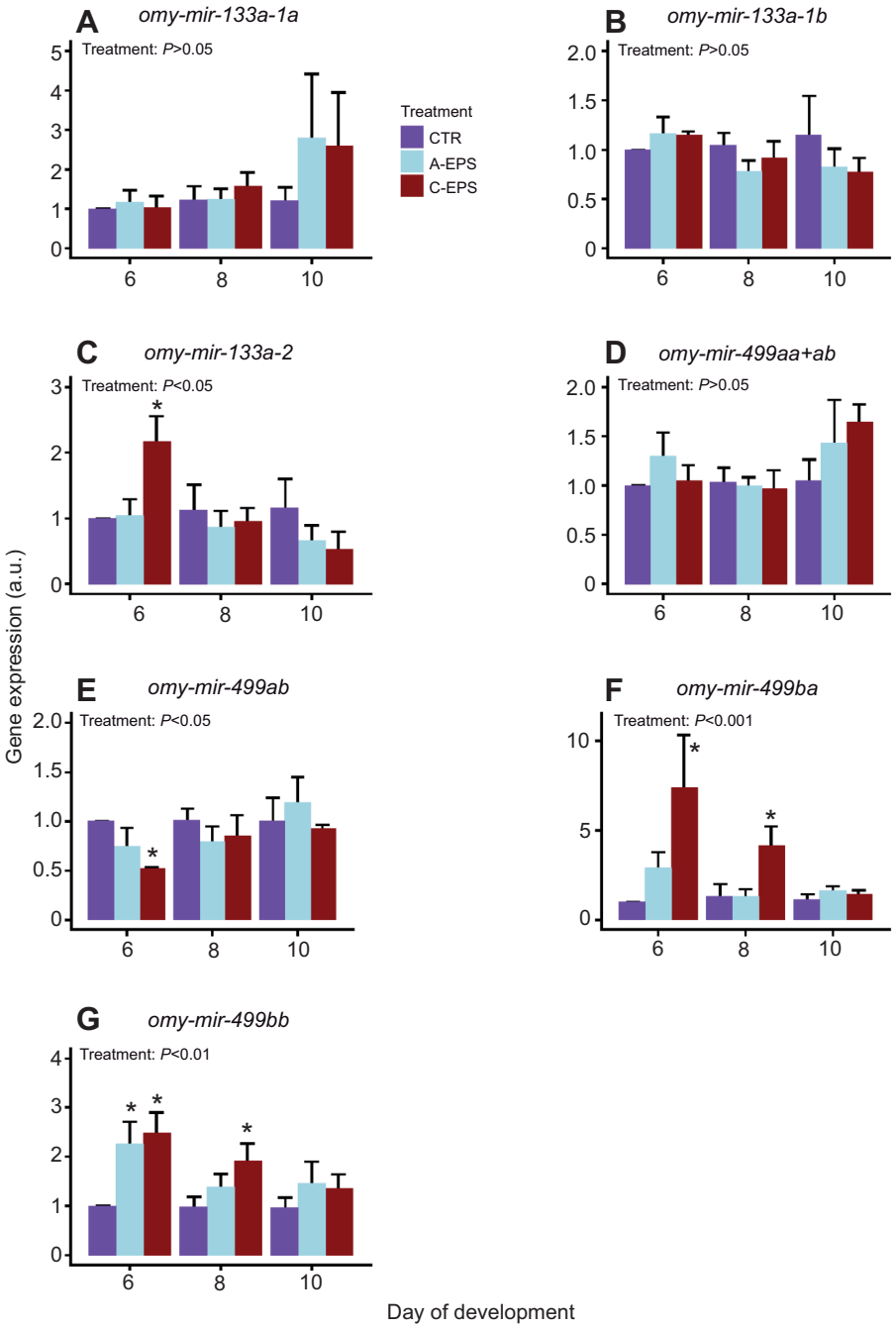

Fig. 7. *miR-133* and *miR-499* paralogue expression in rainbow trout slow myoblast cell culture treated with electrical pulse stimulation (EPS). Gene expression in slow myoblast cell culture at days 6, 8 and 10 of development for (A) *omy-mir-133a-1a*, (B) *omy-mir-133a-1b*, (C) *omy-mir-133a-2*, (D) *omy-mir-499aa+ab*, (E) *omy-mir-499ab*, (F) *omy-mir-499ba* and (G) *omy-mir-499bb*. The treatments are as follows: non-treated myoblasts (CTR, purple bar); myoblasts submitted to acute and high-frequency stimulation (A-EPS, blue bar); and myoblasts submitted to chronic and low-frequency stimulation (C-EPS, red bar). Values represent means±s.e.m. (n=4 independent cell cultures). Data were analyzed using a one-way ANOVA followed by a *post hoc* Dunn's test, with the EPS treatment (treatment) as a factor. P-values of treatment are shown. Asterisks indicate significant differences between means of EPS treatments compared with CTR (P<0.05).

expression and better define their function, which will increase the understanding of how these families regulate fish myogenesis.

Conclusions

We have successfully established a slow myoblast cell culture. The extraction of slow myoblasts opens the doors to future comparative studies between slow and fast muscle development, and regulation, as well as to study the physiology of the slow muscle. We have also characterized the members of the *mir-133* and *mir-499* family in rainbow trout and their expression profiles during myogenesis, confirming the role of *mir-499* in slow muscle phenotype determination and casting doubts about the role of *mir-133* during differentiation. In addition, we have found signs of sub-functionalization of *mir-499* paralogues in response to electrostimulation.

Acknowledgements

We thank Professor Ian Alistair Johnston from the Scottish Oceans Institute (University of St Andrews) for hosting the present research in his laboratory facilities. We also thank Dr Robson Francisco Carvalho and Dr Edson Assunção Mareco for their valuable discussions.

Competing interests

The authors declare no competing or financial interests.

Author contributions

Conceptualization: B.O.D., M.D., D.G.; Methodology: B.O.D., D.G.; Validation: B.O.D., D.G.; Formal analysis: B.O.D., D.G.; Investigation: B.O.D., D.G.; Resources: M.D., D.G.; Data curation: B.O.D., D.G.; Writing - original draft: B.O.D., D.G.; Writing - review & editing: B.O.D., M.D., D.G.; Visualization: B.O.D.; Supervision: M.D., D.G.; Project administration: M.D., D.G.; Funding acquisition: M.D.

Funding

This work received funding from the MASTS pooling initiative (The Marine Alliance for Science and Technology for Scotland) and their support is gratefully acknowledged.

MASTS is funded by the Scottish Funding Council (grant reference HR09011) and contributing institutions. Funding was also provided by the National Council for Scientific and Technological Development (Conselho Nacional de Desenvolvimento Científico e Tecnológico; CNPq), with grants 447233/2014 and 302656/2015-4, and the São Paulo Research Foundation (Fundação de Amparo à Pesquisa do Estado de São Paulo; FAPESP), with grants 2015/03234-8, 2016/19683-9, 2016/05009-4 and 2019/01592-5. The funding agencies did not have roles in the design of the study, analysis of data or writing of manuscript, providing only the financial resources. D.G. is a Serra Húnter Tenure-Track Lecturer of the University of Barcelona.

Data availability

The datasets analyzed for this study can be found in the Ensembl Genome Browser 89 (http://www.ensembl.org/index.html), rainbow trout genome (https://www.genoscope.cns.fr/trout/) (Berthelot et al., 2014), SalmoBase (https://salmobase.org/) (Samy et al., 2017) and NCBI (http://www.ncbi.nlm.nih.gov).

Supplementary information

Supplementary information available online at
http://jeb.biologists.org/lookup/doi/10.1242/jeb.216390.supplemental

References

Andersen, C. L., Jensen, J. L. and Ørntoft, T. F. (2004). Normalization of real-time quantitative reverse transcription-PCR data: a model-based variance estimation approach to identify genes suited for normalization, applied to bladder and colon cancer data sets. *Cancer Res.* **64**, 5245-5250. doi:10.1158/0008-5472.CAN-04-0496

Berthelot, C., Brunet, F., Chalopin, D., Juanchich, A., Bernard, M., Noël, B., Bento, P., Da Silva, C., Labadie, K., Alberti, A. et al. (2014). The rainbow trout genome provides novel insights into evolution after whole-genome duplication in vertebrates. *Nat. Commun.* **5**, 3657. doi:10.1038/ncomms4657

Bessarab, D. A., Chong, S.-W., Srinivas, B. P. and Korzh, V. (2008). Six1a is required for the onset of fast muscle differentiation in zebrafish. *Dev. Biol.* **323**, 216-228. doi:10.1016/j.ydbio.2008.08.015

Bizuayehu, T. T. and Babiak, I. (2014). MicroRNA in teleost fish. *Genome Biol. Evol.* **6**, 1911-1937. doi:10.1093/gbe/evu151

Bone, Q. (1978). Locomotor muscle. In *Fish Physiology: Locomotion*, Vol. VII (ed. W. Hoar and D. Randall), pp. 576. London: Academic Press.

Bower, N. I. and Johnston, I. A. (2010a). Paralogs of Atlantic salmon myoblast determination factor genes are distinctly regulated in proliferating and differentiating myogenic cells. *AJP Regul. Integr. Comp. Physiol.* **298**, R1615-R1626. doi:10.1152/ajpregu.00114.2010

Bower, N. I. and Johnston, I. A. (2010b). Transcriptional regulation of the IGF signaling pathway by amino acids and insulin-like growth factors during myogenesis in Atlantic salmon. *PLoS ONE* **5**, e11100. doi:10.1371/journal.pone.0011100

Box, G. E. P. and Cox, D. R. (1964). An analysis of transformations. *J. R. Stat. Soc. Ser. B* **26**, 211-252. doi:10.1111/j.2517-6161.1964.tb00553.x

Burch, N., Arnold, A.-S., Item, F., Summermatter, S., Brochmann Santana Santos, G., Christe, M., Boutellier, U., Toigo, M. and Handschin, C. (2010). Electric pulse stimulation of cultured murine muscle cells reproduces gene expression changes of trained mouse muscle. *PLoS ONE* **5**, e10970. doi:10.1371/journal.pone.0010970

Bustin, S. A., Benes, V., Garson, J. A., Hellemans, J., Huggett, J., Kubista, M., Mueller, R., Nolan, T., Pfaffl, M. W., Shipley, G. L. et al. (2009). The MIQE guidelines: minimum information for publication of quantitative real-time PCR experiments. *Clin. Chem.* **55**, 611-622. doi:10.1373/clinchem.2008.112797

Castillo, J., Le Bail, P.-Y., Paboeuf, G., Navarro, I., Weil, C., Fauconneau, B. and Gutiérrez, J. (2002). IGF-I binding in primary culture of muscle cells of rainbow trout: changes during *in vitro* development. *Am. J. Physiol. Integr. Comp. Physiol.* **283**, R647-R652. doi:10.1152/ajpregu.00121.2002

Castillo, J., Ammendrup-Johnsen, I., Codina, M., Navarro, I. and Gutiérrez, J. (2006). IGF-I and insulin receptor signal transduction in trout muscle cells. *Am. J. Physiol. Integr. Comp. Physiol.* **290**, R1683-R1690. doi:10.1152/ajpregu.00294.2005

Chan, M. C. and Arany, Z. (2014). The many roles of PGC-1α in muscle – recent developments. *Metabolism* **63**, 441-451. doi:10.1016/j.metabol.2014.01.006

Chen, J.-F., Mandel, E. M., Thomson, J. M., Wu, Q., Callis, T. E., Hammond, S. M., Conlon, F. L. and Wang, D.-Z. (2006). The role of microRNA-1 and microRNA-133 in skeletal muscle proliferation and differentiation. *Nat. Genet.* **38**, 228-233. doi:10.1038/ng1725

Chin, E. R., Olson, E. N., Richardson, J. A., Yang, Q., Humphries, C., Shelton, J. M., Wu, H., Zhu, W., Bassel-Duby, R. and Williams, R. S. (1998). A calcineurin-dependent transcriptional pathway controls skeletal muscle fiber type. *Genes Dev.* **12**, 2499-2509. doi:10.1101/gad.12.16.2499

Cleveland, B. M. and Weber, G. M. (2010). Effects of insulin-like growth factor-I, insulin, and leucine on protein turnover and ubiquitin ligase expression in rainbow trout primary myocytes. *Am. J. Physiol. Integr. Comp. Physiol.* **298**, R341-R350. doi:10.1152/ajpregu.00516.2009

Demetriades, C., Doumpas, N. and Teleman, A. A. (2014). Regulation of TORC1 in response to amino acid starvation via lysosomal recruitment of TSC2. *Cell* **156**, 786-799. doi:10.1016/j.cell.2014.01.024

Drummond, A. J., Suchard, M. A., Xie, D. and Rambaut, A. (2012). Bayesian phylogenetics with BEAUti and the BEAST 1.7. *Mol. Biol. Evol.* **29**, 1969-1973. doi:10.1093/molbev/mss075

Duran, B. O. S., Fernandez, G. J., Mareco, E. A., Moraes, L. N., Salomão, R. A. S., Gutierrez de Paula, T., Santos, V. B., Carvalho, R. F. and Dal-Pai-Silva, M. (2015). Differential microRNA expression in fast- and slow-twitch skeletal muscle of *Piaractus mesopotamicus* during growth. *PLoS ONE* **10**, e0141967. doi:10.1371/journal.pone.0141967

Duran, B. O. S., Góes, G. A., Zanella, B. T. T., Freire, P. P., Valente, J. S., Salomão, R. A. S., Fernandes, A., Mareco, E. A., Carvalho, R. F. and Dal-Pai-Silva, M. (2019). Ascorbic acid stimulates the in vitro myoblast proliferation and migration of pacu (*Piaractus mesopotamicus*). *Sci. Rep.* **9**, 2229. doi:10.1038/s41598-019-38536-4

Fauconneau, B. and Paboeuf, G. (2000). Effect of fasting and refeeding on in vitro muscle cell proliferation in rainbow trout (*Oncorhynchus mykiss*). *Cell Tissue Res.* **301**, 459-463. doi:10.1007/s004419900168

Feldman, J. L. and Stockdale, F. E. (1991). Skeletal muscle satellite cell diversity: satellite cells form fibers of different types in cell culture. *Dev. Biol.* **143**, 320-334. doi:10.1016/0012-1606(91)90083-F

Fujita, H., Nedachi, T. and Kanzaki, M. (2007). Accelerated *de novo* sarcomere assembly by electric pulse stimulation in C2C12 myotubes. *Exp. Cell Res.* **313**, 1853-1865. doi:10.1016/j.yexcr.2007.03.002

Gabillard, J. C., Sabin, N. and Paboeuf, G. (2010). *In vitro* characterization of proliferation and differentiation of trout satellite cells. *Cell Tissue Res.* **342**, 471-477. doi:10.1007/s00441-010-1071-8

Garcia de la serrana, D. and Johnston, I. A. (2013). Expression of heat shock protein (Hsp90) paralogues is regulated by amino acids in skeletal muscle of Atlantic salmon. *PLoS ONE* **8**, e74295. doi:10.1371/journal.pone.0074295

Garcia de la serrana, D., Codina, M., Capilla, E., Jiménez-Amilburu, V., Navarro, I., Du, S.-J., Johnston, I. A. and Gutiérrez, J. (2014a). Characterisation and expression of myogenesis regulatory factors during *in vitro* myoblast development and *in vivo* fasting in the gilthead sea bream (*Sparus aurata*). *Comp. Biochem. Physiol. Part A Mol. Integr. Physiol.* **167**, 90-99. doi:10.1016/j.cbpa.2013.10.020

Garcia de la serrana, D., Mareco, E. A. and Johnston, I. A. (2014b). Systematic variation in the pattern of gene paralog retention between the teleost superorders Ostariophysi and Acanthopterygii. *Genome Biol. Evol.* **6**, 981-987. doi:10.1093/gbe/evu074

Garcia de la serrana, D., Fuentes, E. N., Martin, S. A. M., Johnston, I. A. and Macqueen, D. J. (2017). Divergent regulation of insulin-like growth factor binding protein genes in cultured Atlantic salmon myotubes under different models of catabolism and anabolism. *Gen. Comp. Endocrinol.* **247**, 53-65. doi:10.1016/j.ygcen.2017.01.017

Ge, Y. and Chen, J. (2011). MicroRNAs in skeletal myogenesis. *Cell Cycle* **10**, 441-448. doi:10.4161/cc.10.3.14710

Gibson, M. C. and Schultz, E. (1982). The distribution of satellite cells and their relationship to specific fiber types in soleus and extensor digitorum longus muscles. *Anat. Rec.* **202**, 329-337. doi:10.1002/ar.1092020305

Goljanek-Whysall, K., Sweetman, D. and Münsterberg, A. E. (2012). microRNAs in skeletal muscle differentiation and disease. *Clin. Sci.* **123**, 611-625. doi:10.1042/CS20110634

Gruber, A. R., Lorenz, R., Bernhart, S. H., Neuböck, R. and Hofacker, I. L. (2008). The Vienna RNA websuite. *Nucleic Acids Res.* **36**, W70-W74. doi:10.1093/nar/gkn188

Hagiwara, N., Yeh, M. and Liu, A. (2007). Sox6 is required for normal fiber type differentiation of fetal skeletal muscle in mice. *Dev. Dyn.* **236**, 2062-2076. doi:10.1002/dvdy.21223

Hollway, G. E., Bryson-Richardson, R. J., Berger, S., Cole, N. J., Hall, T. E. and Currie, P. D. (2007). Whole-somite rotation generates muscle progenitor cell compartments in the developing zebrafish embryo. *Dev. Cell* **12**, 207-219. doi:10.1016/j.devcel.2007.01.001

Jaillon, O., Aury, J.-M., Brunet, F., Petit, J.-L., Stange-Thomann, N., Mauceli, E., Bouneau, L., Fischer, C., Ozouf-Costaz, C., Bernot, A. et al. (2004). Genome duplication in the teleost fish Tetraodon nigroviridis reveals the early vertebrate proto-karyotype. *Nature* **431**, 946-957. doi:10.1038/nature03025

Johnston, I. A. (ed.) (2001). Genetic and environmental determinants of muscle growth patterns. In *Muscle Development and Growth*, pp. 141-186. San Diego: Academic Press.

Johnston, I. A. (2006). Environment and plasticity of myogenesis in teleost fish. *J. Exp. Biol.* **209**, 2249-2264. doi:10.1242/jeb.02153

Johnston, I. A., Abercromby, M., Vieira, V. L. A., Sigursteindóttir, R. J., Kristjánsson, B. K., Sibthorpe, D. and Skúlason, S. (2004). Rapid evolution of muscle fiber number in post-glacial populations of Arctic charr *Salvelinus alpinus*. *J. Exp. Biol.* **207**, 4343-4360. doi:10.1242/jeb.01292

Johnston, I. A., Bower, N. I. and Macqueen, D. J. (2011). Growth and the regulation of myotomal muscle mass in teleost fish. *J. Exp. Biol.* **214**, 1617-1628. doi:10.1242/jeb.038620

Kern, M., Wells, J. A., Stephens, J. M., Elton, C. W., Friedman, J. E., Tapscott, E. B., Pekala, P. H. and Dohm, G. L. (1990). Insulin responsiveness in skeletal muscle is determined by glucose transporter (Glut4) protein level. *Biochem. J.* **270**, 397-400. doi:10.1042/bj2700397

Koressaar, T. and Remm, M. (2007). Enhancements and modifications of primer design program Primer3. *Bioinformatics* **23**, 1289-1291. doi:10.1093/bioinformatics/btm091

Kumar, S., Stecher, G. and Tamura, K. (2016). MEGA7: molecular evolutionary genetics analysis version 7.0 for bigger datasets. *Mol. Biol. Evol.* **33**, 1870-1874. doi:10.1093/molbev/msw054

Livak, K. J. and Schmittgen, T. D. (2001). Analysis of relative gene expression data using real-time quantitative PCR and the $2^{-\Delta\Delta Ct}$ method. *Methods* **25**, 402-408. doi:10.1006/meth.2001.1262

Ma, G., Wang, Y., Li, Y., Cui, L., Zhao, Y., Zhao, B. and Li, K. (2015). MiR-206, a key modulator of skeletal muscle development and disease. *Int. J. Biol. Sci.* **11**, 345-352. doi:10.7150/ijbs.10921

Macqueen, D. J. and Johnston, I. A. (2014). A well-constrained estimate for the timing of the salmonid whole genome duplication reveals major decoupling from species diversification. *Proc. Biol. Sci.* **281**, 20132881. doi:10.1098/rspb.2013.2881

Macqueen, D. J., Kristjánsson, B. K. and Johnston, I. A. (2010). Salmonid genomes have a remarkably expanded akirin family, coexpressed with genes from conserved pathways governing skeletal muscle growth and catabolism. *Physiol. Genomics* **42**, 134-148. doi:10.1152/physiolgenomics.00045.2010

Macqueen, D. J., Garcia de la serrana, D. and Johnston, I. A. (2013). Evolution of ancient functions in the vertebrate insulin-like growth factor system uncovered by study of duplicated salmonid fish genomes. *Mol. Biol. Evol.* **30**, 1060-1076. doi:10.1093/molbev/mst017

Maere, S. and Van de Peer, Y. (2010). Duplicate retention after small- and large-scale duplications. In *Evolution after Gene Duplication* (ed. K. Dittmar and D. Liberles), pp. 329. Hoboken, NJ: John Wiley & Sons.

Marotta, M., Bragós, R. and Gómez-Foix, A. M. (2004). Design and performance of an electrical stimulator for long-term contraction of cultured muscle cells. *BioTechniques* **36**, 68-73. doi:10.2144/04361ST01

McCarthy, J. J. (2011). The MyomiR network in skeletal muscle plasticity. *Exerc. Sport Sci. Rev.* **39**, 150-154. doi:10.1097/JES.0b013e31821c01e1

McCarthy, J. J., Esser, K. A., Peterson, C. A. and Dupont-Versteegden, E. E. (2009). Evidence of MyomiR network regulation of β-myosin heavy chain gene expression during skeletal muscle atrophy. *Physiol. Genomics* **39**, 219-226. doi:10.1152/physiolgenomics.00042.2009

Montserrat, N., Gabillard, J. C., Capilla, E., Navarro, M. I. and Gutiérrez, J. (2007a). Role of insulin, insulin-like growth factors, and muscle regulatory factors in the compensatory growth of the trout (*Oncorhynchus mykiss*). *Gen. Comp. Endocrinol.* **150**, 462-472. doi:10.1016/j.ygcen.2006.11.009

Montserrat, N., Sánchez-Gurmaches, J., Garcia de la Serrana, D., Navarro, M. I. and Gutiérrez, J. (2007b). IGF-I binding and receptor signal transduction in primary cell culture of muscle cells of gilthead sea bream: changes throughout *in vitro* development. *Cell Tissue Res.* **330**, 503-513. doi:10.1007/s00441-007-0507-2

Nachtigall, P. G., Dias, M. C., Carvalho, R. F., Martins, C. and Pinhal, D. (2015). MicroRNA-499 expression distinctively correlates to target genes sox6 and rod1 profiles to resolve the skeletal muscle phenotype in Nile tilapia. *PLoS ONE* **10**, e0119804. doi:10.1371/journal.pone.0119804

Nedachi, T., Fujita, H. and Kanzaki, M. (2008). Contractile C_2C_{12} myotube model for studying exercise-inducible responses in skeletal muscle. *Am. J. Physiol. Metab.* **295**, E1191-E1204. doi:10.1152/ajpcell.00144.2008

Nikolić, N., Skaret Bakke, S., Tranheim Kase, E., Rudberg, I., Flo Halle, I., Rustan, A. C., Thoresen, G. H. and Aas, V. (2012). Electrical pulse stimulation of cultured human skeletal muscle cells as an in vitro model of exercise. *PLoS ONE* **7**, e33203. doi:10.1371/journal.pone.0033203

Olson, E. N. and Williams, R. S. (2000). Calcineurin signaling and muscle remodeling. *Cell* **101**, 689-692. doi:10.1016/S0092-8674(00)80880-6

Rossi, G. and Messina, G. (2014). Comparative myogenesis in teleosts and mammals. *Cell. Mol. Life Sci.* **71**, 3081-3099. doi:10.1007/s00018-014-1604-5

Samy, J. K. A., Mulugeta, T. D., Nome, T., Sandve, S. R., Grammes, F., Kent, M. P., Lien, S. and Våge, D. I. (2017). SalmoBase: an integrated molecular data resource for Salmonid species. *BMC Genomics* **18**, 482. doi:10.1186/s12864-017-3877-1

Sancak, Y., Bar-Peled, L., Zoncu, R., Markhard, A. L., Nada, S. and Sabatini, D. M. (2010). Ragulator-rag complex targets mTORC1 to the lysosomal surface and is necessary for its activation by amino acids. *Cell* **141**, 290-303. doi:10.1016/j.cell.2010.02.024

Sandri, M. (2008). Signaling in muscle atrophy and hypertrophy. *Physiology* **23**, 160-170. doi:10.1152/physiol.00041.2007

Sänger, A. M. and Stoiber, W. (2001). Muscle fiber diversity and plasticity. In *Muscle Development and Growth* (ed. I. A. Johnston), pp. 187-250. San Diego: Academic Press.

Schiaffino, S. and Reggiani, C. (2011). Fiber types in mammalian skeletal muscles. *Physiol. Rev.* **91**, 1447-1531. doi:10.1152/physrev.00031.2010

Seger, C., Hargrave, M., Wang, X., Chai, R. J., Elworthy, S. and Ingham, P. W. (2011). Analysis of Pax7 expressing myogenic cells in zebrafish muscle development, injury, and models of disease. *Dev. Dyn.* **240**, 2440-2451. doi:10.1002/dvdy.22745

Seiliez, I., Gabillard, J.-C., Skiba-Cassy, S., Garcia-Serrana, D., Gutiérrez, J., Kaushik, S., Panserat, S. and Tesseraud, S. (2008). An *in vivo* and *in vitro* assessment of TOR signaling cascade in rainbow trout (*Oncorhynchus mykiss*). *AJP Regul. Integr. Comp. Physiol.* **295**, R329-R335. doi:10.1152/ajpregu.00146.2008

Silveira, L. R., Pilegaard, H., Kusuhara, K., Curi, R. and Hellsten, Y. (2006). The contraction induced increase in gene expression of peroxisome proliferator-activated receptor (PPAR)-γ coactivator 1α (PGC-1α), mitochondrial uncoupling protein 3 (UCP3) and hexokinase II (HKII) in primary rat skeletal muscle cells is dependent on reactive oxygen species. *Biochim. Biophys. Acta Mol. Cell Res.* **1763**, 969-976. doi:10.1016/j.bbamcr.2006.06.010

Thelen, M. H., Simonides, W. S. and van Hardeveld, C. (1997). Electrical stimulation of C_2C_{12} myotubes induces contractions and represses thyroid-hormone-dependent transcription of the fast-type sarcoplasmic-reticulum Ca^{2+}-ATPase gene. *Biochem. J.* **321**, 845-848. doi:10.1042/bj3210845

Untergasser, A., Cutcutache, I., Koressaar, T., Ye, J., Faircloth, B. C., Remm, M. and Rozen, S. G. (2012). Primer3 – new capabilities and interfaces. *Nucleic Acids Res.* **40**, e115. doi:10.1093/nar/gks596

van Rooij, E., Liu, N. and Olson, E. N. (2008). MicroRNAs flex their muscles. *Trends Genet.* **24**, 159-166. doi:10.1016/j.tig.2008.01.007

van Rooij, E., Quiat, D., Johnson, B. A., Sutherland, L. B., Qi, X., Richardson, J. A., Kelm, R. J. and Olson, E. N. (2009). A family of microRNAs encoded by myosin genes governs myosin expression and muscle performance. *Dev. Cell* **17**, 662-673. doi:10.1016/j.devcel.2009.10.013

Vélez, E. J., Lutfi, E., Jiménez-Amilburu, V., Riera-Codina, M., Capilla, E., Navarro, I. and Gutiérrez, J. (2014). IGF-I and amino acids effects through TOR signaling on proliferation and differentiation of gilthead sea bream cultured myocytes. *Gen. Comp. Endocrinol.* **205**, 296-304. doi:10.1016/j.ygcen.2014.05.024

Vélez, E. J., Lutfi, E., Azizi, S., Montserrat, N., Riera-Codina, M., Capilla, E., Navarro, I. and Gutiérrez, J. (2016). Contribution of *in vitro* myocytes studies to understanding fish muscle physiology. *Comp. Biochem. Physiol. Part B Biochem. Mol. Biol.* **199**, 67-73. doi:10.1016/j.cbpb.2015.12.003

von Hofsten, J., Elworthy, S., Gilchrist, M. J., Smith, J. C., Wardle, F. C. and Ingham, P. W. (2008). Prdm1- and Sox6-mediated transcriptional repression specifies muscle fiber type in the zebrafish embryo. *EMBO Rep.* **9**, 683-689. doi:10.1038/embor.2008.73

Wang, X., Ono, Y., Tan, S. C., Chai, R. J., Parkin, C. and Ingham, P. W. (2011). Prdm1a and miR-499 act sequentially to restrict Sox6 activity to the fast-twitch muscle lineage in the zebrafish embryo. *Development* **138**, 4399-4404. doi:10.1242/dev.070516

Wickham, H. (2016). *ggplot2: Elegant Graphics for Data Analysis*, 2nd edn. New York: Springer-Verlag.

Yu, H., Lu, Y., Li, Z. and Wang, Q. (2014). microRNA-133: expression, function and therapeutic potential in muscle diseases and cancer. *Curr. Drug Targets* **15**, 817-828. doi:10.2174/1389450115666140627104151

Table S1: Precursor miRNA sequences of each species used in the analyses and their respective nomenclature according to the evolutionary relationship provided by the Bayesian phylogenetic trees.

Click here to Download Table S1

Table S2: Quantitative PCR primer sequences. Genes are as follow: *slow myhc* (*slow myosin heavy chain*); *fast myhc* (*fast myosin heavy chain*); *sox6* (*(sex determining region Y)-box 6*); *six1* (*six homeobox 1*); *glut4* (*insulin-responsive glucose transporter type 4*); *lamtor3* (*late endosomal/lysosomal adaptor, mapk and mtor activator 3*); *ragd* (*ras related GTP binding D*); *rptor* (*regulatory associated protein of mtor complex 1*); *mafbx* (*muscle atrophy f-box protein*); *pgc1α* (*peroxisome proliferator-activated receptor gamma coactivator 1 alpha*); *ckma* (*creatine kinase, m-type a*); *ckmb* (*creatine kinase, m-type b*); *myog* (*myogenin*); *rpl13* (*ribosomal protein L13*); *rpl19* (*ribosomal protein L19*); *omy-mir-133a-1a*, *omy-mir-133a-1b*, *omy-mir- 133a-2* (precursor sequences of rainbow trout mir-133 paralogues); *omy-mir-499aa+ab*, *omy-mir-499ab*, *omy-mir-499ba*, *omy-mir-499bb* (precursor sequences of rainbow trout mir-499 paralogues); *omy-mir-206-1* (precursor sequence of rainbow trout mir-206); and *U6 snRNA* (*U6 small nuclear RNA*). Accession code based on rainbow trout genome in Genoscope (https://www.genoscope.cns.fr/trout/) (Berthelot et al., 2014) or NCBI (http://www.ncbi.nlm.nih.gov) database.

Gene	Primers (5’ to 3’)	Tm (°C)	Accession code
slow myhc	F: AGTTCCGCAAGATTCAGCAT R: GCCGACATCACAACTCTTGA	81	AF211172.1
fast myhc	F: GGCCAAGAAGGCTATCACTG R: GCCAGATTCTCAGCCTCATC	84	Z48794.1
sox6	F: TGGGAGAGGATGATGGAAAG R: CCCAGGATCTTGCTGATGTT	85	XM_021566535.1
six1	F: TCCCTCTGGATATCGGCGTT R: AGAAAACGACCGAGCCTCTC	83	XM_021574266.1
glut4	F: GTGCCAGGCTTATTGTCCATATTC R: TAGAGAAGATGGCCACCGACAG	85	XM_021615262.1
lamtor3	F: TCACCATGGACTGGGGGTTA R: TGCGTTATCATTTGCCACTTTG	79	NM_001160681.1
ragd	F: AGGGGGTTTCGAAGTACACC R: TGAAACCACCTCCGTCTTCG	80	XM_021573884.1
rptor	F: CCATCGACAAGATGAGACGA R: CCTGGGGAGACAGAGACAGA	86	XM_021557184.1
mafbx	F: CAGGAGCCCGAGTGACTTTT R: ATCAAATGCACCATCACCCCT	76	NM_001193326.1
pgc1α	F: AACCTGAGAGATGACGGGGA R: GTGTGTCCGTTTTCAAGGGC	78	XM_021617116.1
ckma	F: GTGGGTGGAGTGTTCGACAT R: TCCACCATGAGCTTGACACC	82	XM_021623857.1
ckmb	F: AGCACACACCCCAAGTTTGA R: CAGAAGATCCCAGACGGTCA	84	XM_021617754.1

myog	F: AGCAACACCTCAGACCACTG R: AGGAGGTCCTCGTTGCTGTA	75	NM_001124727.1
rpl13	F: CACCATTGGCATCTCTGTTG R: AGTGCTGTCTCCCTTCTTGG	85	scaffold_1560 chrUn_26:11288161..11308160
rpl19	F: GAGAAGACGACGCAGGATTC R: CAAGTGAAGGCACACAGGAA	80	scaffold_1008 chrUn_1:27789918..27809917
omy-mir-133a-1a	F: AGTGAACCCCCAATGCTTT R: GGGACCAAATCCATTCAAGA	73	scaffold_1560 chrUn:390576274..390581273
omy-mir-133a-1b	F: GACAAACACCTAATGCCTTG R: GGGACCAAATCCATTCAAGA	73	scaffold_79929 chrUn:366226605..366231604
omy-mir-133a-2	F: TTCACACCAAAAATGCTTT R: GGGACCAAATCCATTGAACA	71	scaffold_1154 chrUn:346363877..346368876
omy-mir-499aa+ab	F: CTGAGAAGGAGACAGTTAAGACTTG R: AGAGTGGAGCCAGCAGAGAC	74	scaffold_984 chrUn_17:42432554..42452553
omy-mir-499ab	F: AGGAGACAGTTAAGACTTGC R: TGAGAATGGAGCCAGCAC	74	scaffold_116 chrUn_7:18225955..18230954
omy-mir-499ba	F: GAGGGAAGTAGTTAAGACTTG R: CTTAAAGTGATGTTCATGAGT	70	scaffold_347 chrUn_9:20331061..20336060
omy-mir-499bb	F: GAGGGAAGTAGTTAAGACTTA R: CTTAAAGTGATGTTCATGAGC	70	scaffold_1915 chrUn_16:304245..309244
omy-mir-206-1	F: TCGTTGCCTCCTGTGAAGAC R: CTCCATTCCCCTTGTAACCA	76	scaffold_13810 chrUn:893645720..893645918
U6 snRNA	F: GGCTTCGGCAGCACATATAC R: AACGCTTCACGATTTTGC	77	scaffold_15039 chrUn:278113300..278133299

Tm, melting temperature; F, forward; R, reverse.

Table S3: Rainbow trout miRNAs similarity. Percentage of similarity between miRNAs paralogues identified in rainbow trout.

Paralogue	Nucleotide similarity
omy-mir-133a-1a vs *omy-mir-133a-1b*	97%
omy-mir-133a-1a vs *omy-mir-133a-2*	93%
omy-mir-133a-1b vs *omy-mir-133a-2*	92%
omy-mir-499aa vs *omy-mir-499ab*	96%
omy-mir-499ba vs *omy-mir-499bb*	97%

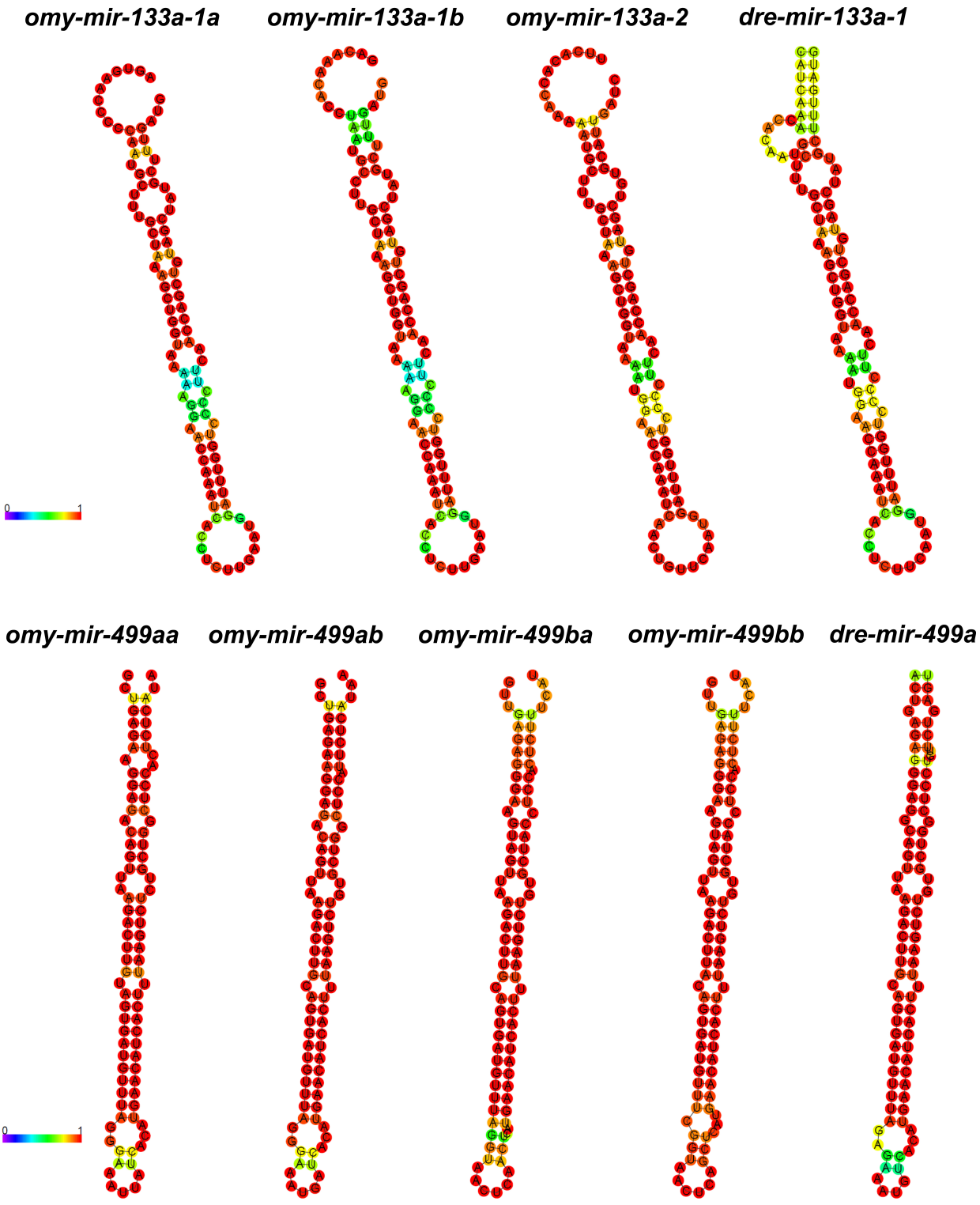

Figure S1: Predicted secondary structures of the identified miRNA precursor sequences. The precursor sequences of the mir-133 and mir-499 paralogues were submitted to minimum free energy (MFE) prediction of the optimal secondary structures in dot-bracket notation. Base pair probabilities are color coded 0-1, with higher numbers corresponding to higher confidence. Secondary structures of zebrafish *dre-mir-133a-1* and *dre-mir-499a* precursor sequences are shown only for comparative purposes.

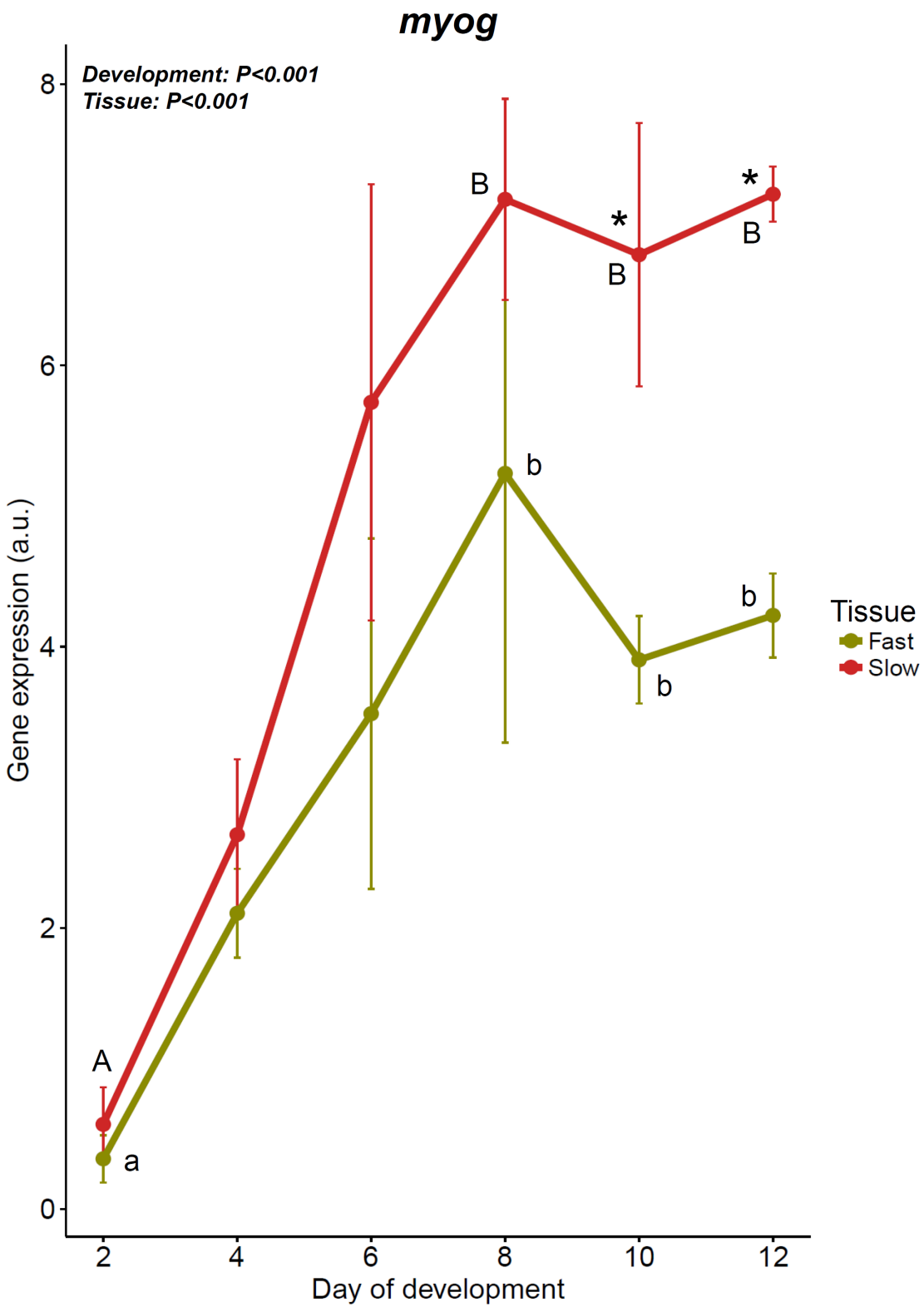

Figure S2: *Myogenin* expression in rainbow trout fast and slow myoblast cell culture.

Myogenin (*myog*) expression in slow and fast myoblast cell culture at days 2, 4, 6, 8, 10 and 12 of development. Values represent mean ± SE (n=4 independent cell cultures; a.u.= arbitrary units). The P-values of the tissue of origin (*tissue*) and the day of development (*development*) are shown in the left corner of the graph. Asterisks indicate significant differences between means of slow myoblasts and fast myoblasts cell cultures, and different letters (upper case for slow and lower case for fast) indicate significant differences between means of days of development (P<0.05).

A

Correlation	133a1a	133a1b	133a2	499aa +ab	499ab	499ba	499bb	*smyhc*	*fmyhc*	*sox6*
133a1a	1	0,21	0,11	0,2	0,12	0,02	0,17	-0,12	-0,02	0,26
133a1b		1	0,55***	-0,1	0,16	0,14	0,09	-0,2	0,55***	0,4**
133a2			1	-0,1	-0,05	0,27	0,21	0,02	0,26	0,13
499aa+ab				1	0,71***	0,11	0,6***	0,26	-0,17	-0,38*
499ab					1	0,13	0,41**	0,46**	0,21	-0,27
499ba						1	0,69***	0,15	-0,24	-0,5**
499bb							1	0,08	-0,31*	-0,51***
smyhc								1	0,19	-0,46**
fmyhc									1	0,45**
sox6										1

B

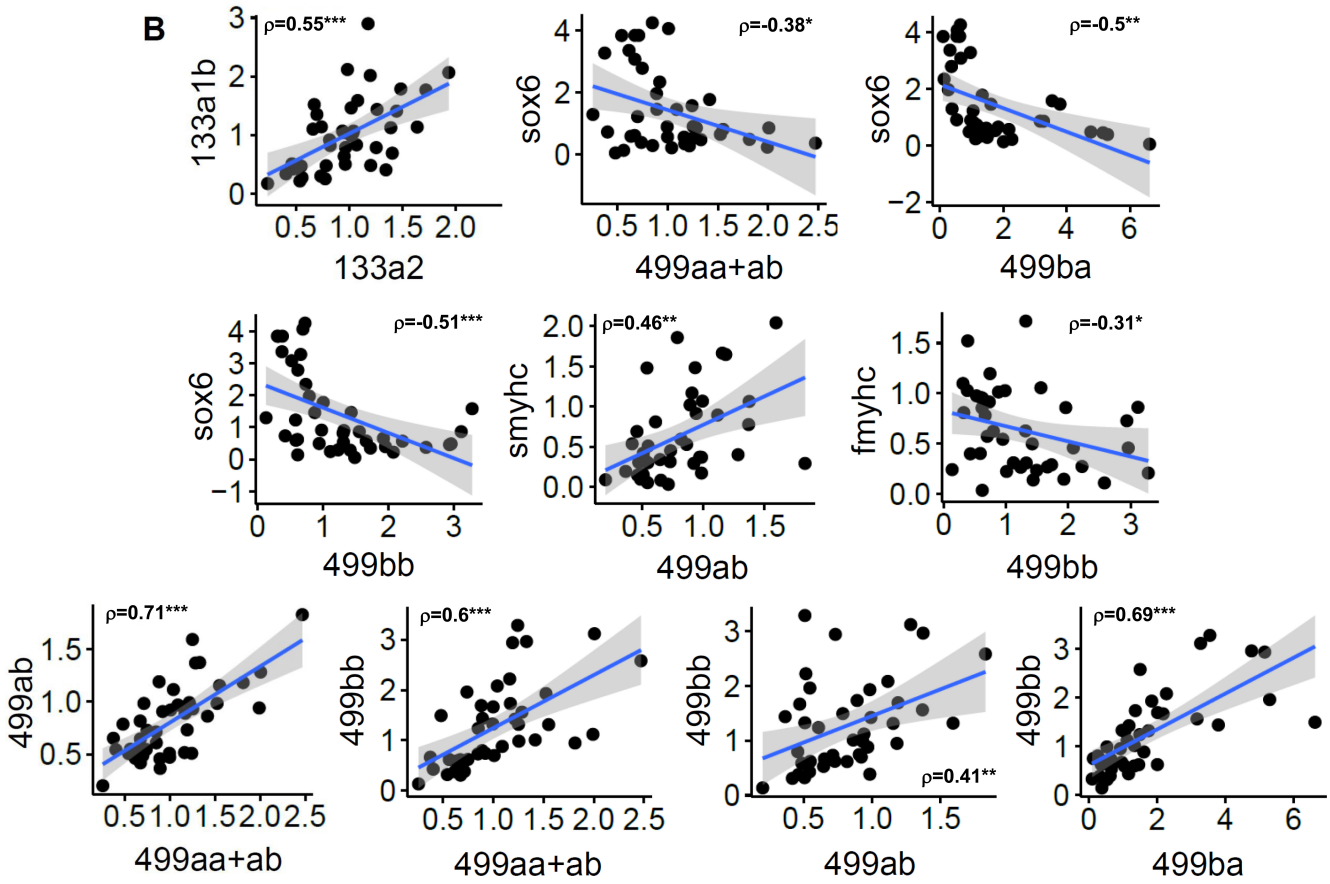

Figure S3: Correlation of rainbow trout miRNAs and mRNAs expression. (A) Pearson's correlation (ρ) index between the expression of *omy-mir-133* and *omy-mir-499* paralogues, and *smyhc*, *fmyhc* and *sox6* mRNAs. (B) Plot char between gene expression values for *omy-mir-133a-1b* vs *omy-mir-133a-2*, *omy-mir-499aa+ab* vs *sox6*, *omy-mir-499ba* vs *sox6*, *omy-mir-499bb* vs *sox6*, *omy-mir-499ab* vs *smyhc*, *omy-mir-499bb* vs *fmyhc*, *omy-mir-499aa+ab* vs *omy-mir-499ab*, *omy-mir-499aa+ab* vs *omy-mir-499bb*, *omy-mir-499ab* vs *omy-mir-499bb* and *omy-mir-499ba* vs *omy-mir-499bb*. Pearson correlation and p-value are indicated in the corners of the plot graphs. Significant differences between gene correlations are indicated with one (P<0.05), two (P<0.01) or three (P<0.001) asterisks.